nature protocols

PROTOCOL

https://doi.org/10.1038/s41596-019-0239-2

# Imaging neuromodulators with high spatiotemporal resolution using genetically encoded indicators

Tommaso Patriarchi[1,6], Jounhong Ryan Cho[2], Katharina Merten[3], Aaron Marley[4], Gerard Joey Broussard[1,7], Ruqiang Liang[1], John Williams[5*], Axel Nimmerjahn[3*], Mark von Zastrow[4*], Viviana Gradinaru[2*] and Lin Tian[1*]

**Multiple aspects of neural activity, from neuronal firing to neuromodulator release and signaling, underlie brain function and ultimately shape animal behavior. The recently developed and constantly growing toolbox of genetically encoded sensors for neural activity, including calcium, voltage, neurotransmitter and neuromodulator sensors, allows precise measurement of these signaling events with high spatial and temporal resolution. Here, we describe the engineering, characterization and application of our recently developed dLight1, a suite of genetically encoded dopamine (DA) sensors based on human inert DA receptors. dLight1 offers high molecular specificity, requisite affinity and kinetics and great sensitivity for measuring DA release in vivo. The detailed workflow described in this protocol can be used to systematically characterize and validate dLight1 in increasingly intact biological systems, from cultured cells to acute brain slices to behaving mice. For tool developers, we focus on characterizing five distinct properties of dLight1: dynamic range, affinity, molecular specificity, kinetics and interaction with endogenous signaling; for end users, we provide comprehensive step-by-step instructions for how to leverage fiber photometry and two-photon imaging to measure dLight1 transients in vivo. The instructions provided in this protocol are designed to help laboratory personnel with a broad range of experience (at the graduate or post-graduate level) to develop and utilize novel neuromodulator sensors in vivo, by using dLight1 as a benchmark.**

## Introduction

Neural communication relies on the production and release of neurotransmitter and neuromodulatory molecules in the extracellular space. Once released, these molecules bind to and activate their cognate receptors on the membranes of the receiving cells. This in turn triggers downstream signaling cascades that can profoundly alter connectivity and the firing patterns of local microcircuits[1–3]. Because the amount of time a neuromodulator spends in the extracellular space directly relates to its downstream actions, the ability to measure the extracellular dynamics of specific neuromodulators and correlate them with animal behavior or disease states becomes essential to understanding their mechanisms of action[4,5].

For decades, the only resources available for measuring extracellular fluctuations of neuromodulators were provided by analytical chemistry techniques[6], which include electrochemical methods (amperometry and fast-scan cyclic voltammetry)[7] and microdialysis[8]. Although electrochemical methods can achieve fast (subsecond) and quantitative readouts, they can provide only point measurements and rely on background subtraction, which prevents detection of prolonged changes in transmitter levels[9]. These techniques also lack the required molecular specificity necessary to identify individual neuromodulators and distinguish them from their metabolites (e.g., DA, norepinephrine, 3,4-dihydroxyphenylacetic acid)[10]. On the other hand, microdialysis, especially when coupled with HPLC-mass spectrometry (HPLC-MS) detection, offers

[1]Department of Biochemistry and Molecular Medicine, University of California, Davis, Davis, CA, USA. [2]Division of Biology and Biological Engineering, California Institute of Technology, Pasadena, CA, USA. [3]Waitt Advanced Biophotonics Center, Salk Institute for Biological Studies, La Jolla, CA, USA. [4]Department of Cellular and Molecular Pharmacology, University of California, San Francisco, San Francisco, CA, USA. [5]Vollum Institute, Oregon Health & Science University, Portland, OR, USA. [6]Present address: Institute of Pharmacology and Toxicology, University of Zurich, Zurich, Switzerland. [7]Present address: Princeton Neuroscience Institute and Department of Molecular Biology, Princeton University, Princeton, NJ, USA.
*e-mail: williamj@ohsu.edu; animmerj@salk.edu; mark@vzlab.org; viviana@caltech.edu; lintian@ucdavis.edu

great molecular specificity but has a coarse time resolution (usually on the order of minutes) due to dialysate collection times[11].

As an alternative to these techniques, cell-based (cell-based neurotransmitter fluorescent engineered reporters (CNiFERs))[12] and reporter gene expression-based (iTango2)[13] systems have been introduced in recent years. Both systems rely on the use of G-protein-coupled receptors (GPCRs) for sensing the molecule of interest and thus can afford high molecular specificity. However, CNiFERs report neuromodulator dynamics indirectly, by coupling GPCR activation to intracellular $Ca^{2+}$ detection via a Förster resonance energy transfer (FRET)-based calcium sensor, stably expressed in an immortalized cell line. As a result, this system is inherently slow (temporal resolution of 5 s) and has limited sensitivity, due to the small fractional change of FRET-based sensors. The iTango2 system, on the other hand, works by coupling light and ligand-dependent activation of a GPCR construct tethered to an orthogonal transcription factor. In this case, the temporal resolution is limited by gene expression times and thus cannot be used for real-time measurements.

To enable direct and specific measurement of diverse types of neuromodulators with the necessary spatiotemporal resolution, it is advantageous to design a sensor with molecular specificity, affinity and kinetics similar to those of endogenous receptors. Because GPCRs are native neuromodulator targets, we have pioneered a new approach for biosensor design based on protein engineering of the cognate GPCRs. We demonstrated that by engineering a circularly permuted green fluorescent protein (cpGFP), upon which widely utilized genetically encoded calcium indicators (GCaMPs) are built[14,15], directly into inert human DA receptors, it is possible to directly transform receptor activation in a fluorescent observable, thus providing an optical readout of DA transients[16]. The dLight1 family consists of six sensors based on three DA receptors (DRD1, DRD2 and DRD4) with broadly tunable affinity and dynamic range and the ability probe DA transients across the nanomolar–millimolar range of concentrations. In addition, we further extended the design strategy to engineer sensors for any desired neuromodulators or pharmacological drugs on a subset of GPCRs (either Gs, Gi or Gq coupled). Because all class A (rhodopsin-like) GPCRs share a common activation mechanism[17,18], by replacing the third intracellular loop of the receptor with the 'universal cpGFP module'[16], we obtained preliminary GPCR-sensor variants that respond to their endogenous ligands, including serotonin, norepinephrine, melatonin and opioid peptides, with positive fluorescence changes, although the dynamic range of the response ($\Delta F/F$) is variable among different GPCRs[16] (Supplementary Fig. 1).

In this protocol, using dLight1 as an example, we first outline the steps necessary to optimize and characterize the intrinsic properties of neuromodulator sensors, which need to be fine-tuned each time a new sensor is developed and tailored to the specific experimental conditions of use. We then provide instructions for validating their use in awake, behaving animals in combination with fiber photometry or two-photon imaging, offering an easy solution for tracking the dynamics of neuromodulatory molecules during complex behaviors or disease states.

## Overview of the procedure

Although GPCR-based sensor design leads to the development of prototype sensors for any given ligand, the procedure for sensor optimization is often serendipitous and needs to be addressed on a case-by-case basis. Here, we provide a general strategy on how to attempt sensor optimization (Fig. 1). The first optimization stage during the screening process focuses on improving two critical parameters: dynamic range and affinity (Steps 1–6). For instance, shifting the insertion site of the cpGFP module along the sequence connecting transmembrane helixes 5 and 6 of the GPCR has been shown to affect membrane expression and has been used to modify the dynamic range and affinity of dLight1 (ref. [16]). It is possible that continued development and optimization of these probes, as well as performing structural studies on them, may lead to useful insights into their activation mechanisms and thus provide more accurate guidance on how to rationally improve their properties.

We next focus on describing in detail the methods required for the characterization and validation of newly developed GPCR-based genetically encoded sensors in increasingly intact biological systems, from cultured cells (Steps 7–23) to brain slices (Steps 24–35A) to awake, behaving mice (Step 35B–D) (Fig. 2). Importantly, the experimental conditions (i.e., brain region of interest (ROI), pharmacological and/or optogenetic manipulations) for both ex vivo and in vivo validation need to be modified to reflect the specific physiological characteristics of the neuromodulatory system under investigation.

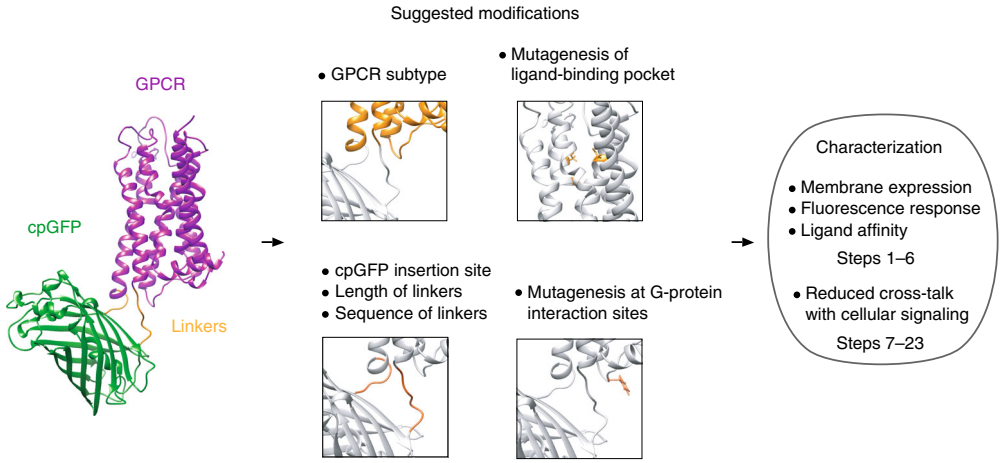


**Fig. 1 | General strategy for GPCR-based sensor development.** Left, structural model of dLight1 (ref. [16]), illustrating the components of genetically encoded GPCR sensors: circularly permutated green fluorescent protein (green), amino acid linkers (orange) and GPCR moiety (purple). Center, possible approaches to sensor development are indicated. Sensor components subject to possible modification are highlighted in orange in the structural model closeups. Right, procedures required to establish the effects of the engineered modifications on sensor performance. These include characterization of sensor performance (Steps 1–6) and interaction with intracellular signaling (Steps 7–23).

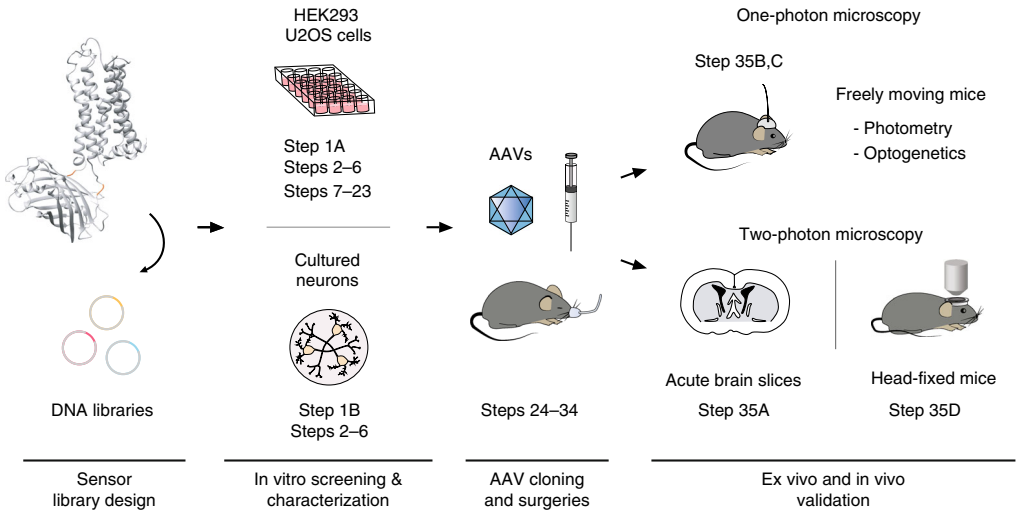


**Fig. 2 | Outline of the workflow for sensor characterization and validation.** The procedures outlined here start from simpler eukaryotic systems and gradually move to increasingly complex mammalian systems. Various mutagenesis approaches can be used to alter the sequence of the sensor according to the design strategy chosen by the user. The extracted DNA can then be transfected into mammalian cell lines or transduced into primary cultured neurons to characterize sensor properties in vitro. These steps (Steps 1–23) will lead to the identification of a top-performing sensor variant. The next steps (Steps 24–34) describe the procedures related to the animal surgeries necessary for in vivo experiments. The last step (Step 35A–D) describes the procedures for ex vivo and in vivo validation of the sensor. The kinetics and pharmacological properties of the sensor will be first determined in brain slices under two-photon microscopy (Step 35A). Subsequently, fiber photometry imaging, alone or in combination with optogenetic manipulations, will be used to validate sensor function in vivo (Step 35B,C). Finally, two-photon microscopy will be used to study dopamine release in the cortex of head-fixed mice (Step 35D).

## Limitations of the tools

Genetically encoded sensors are constructed based on fluorescent proteins (FPs) and thus inherit both benefits and limitations of their optical properties, such as spectral bandwidth, maximal brightness, pH sensitivity and photostability. Although intensity-based sensors, such as dLight1, benefit from large fluorescence responses and preserved spectral bandwidth, which allows the coupling with

spectrally orthogonal optogenetic reporters or actuators[16], it is important to keep in mind that they are not ratiometric and thus cannot be accurately calibrated to measure absolute DA concentrations in vivo. For applications in which a determination of the absolute concentration of DA release is necessary, the use of fast-scan cyclic voltammetry or microdialysis[11] is preferred over use of fluorescent sensors. In addition, absorption cross-section and fluorescence response amplitude of a sensor can differ greatly when measured under one-photon and two-photon microscopy, which should be properly addressed during sensor development and characterization. Low baseline fluorescence is especially important for wide-field imaging, in which much larger tissue volumes contribute to the background[19,20]. In general, the signal-to-noise ratio (SNR) in two-photon imaging can be increased by reducing the background fluorescence, especially in neuropils, with two alternative approaches, depending on the experimental conditions and types of sensors being used: (i) targeting the sensor specifically to subcellular locations, such as sparse labeling of a neuronal population[21], somatic membrane targeting for voltage/calcium sensors[22] and axonal targeting for calcium sensors[23]; (ii) using probes with a lower baseline fluorescence but with large a dynamic range when targeting is difficult. An example of this can be seen in the comparison of dLight1.1 with dLight1.2 under two-photon in vivo imaging from the dorsal striatum (Supplementary Fig. 2). In this case, the relatively lower baseline and higher apparent affinity of dLight1.1 presumably contribute to a higher response as compared to that of dLight1.2 in both two-photon and fiber photometry imaging, although the dynamic range of dLight1.1 determined in situ in HEK293 cells was lower compared to that of dLight1.2.

Another potential limitation of these tools that needs to be considered is the potential interference of the probe with endogenous signaling pathways. To address this issue, a systematic characterization of the physiological properties of cells and circuits with and without sensor expression is highly recommended. For example, depending on the receptor type (whether it is Gs, Gi or Gq coupled), different cell-based assays can be used to investigate, for instance, the effect of sensor expression on endogenous cAMP production or β-arrestin-dependent sensor internalization[16]. In addition, depending on the relationship between analyte concentration and indicator concentration and volume, buffering effects (i.e., alterations in the sensitivity of sensor-expressing cells to the action of the neuromodulator) are possible, and these need to be controlled for by measuring the effect of sensor expression on cAMP production in a cell type that endogenously expresses the receptor used for sensor engineering (i.e., U2OS cells in the case of dLight1-type sensors; Steps 19–23).

### Considerations for sensor developers

The sensor engineering process, broadly defined as any modification intentionally introduced into the amino acid sequence of a sensor, will affect important properties of the probes, such as their membrane expression, ligand-binding affinity, molecular specificity, dynamic range, kinetics and interaction with endogenous signaling. To allow easy implementation of sensors, it is important to start with a systematic characterization of their properties in vitro. For maximal sensitivity, sensors with large positive fluorescence changes upon ligand binding are preferred. Depending on the type of neuromodulator sensor being developed, engineering efforts can next focus on fine-tuning the affinity of the sensor to match the physiological concentrations of neuromodulator released in vivo. Taking dLight1 sensors as an example, it seems that during probe development, the dynamic range and affinity of the probes stand in an inverse relationship, with increases in one property being detrimental to the other. We speculate that this is due to constraints imparted on the conformational flexibility of the GPCR by the engineered FP module. Through engineering GCaMP[15], iGluSnFR[24] and dLight1 (ref. [16]), we learned that both linker regions between the ligand-binding proteins and cpGFP are critical to a sensor's dynamic range. Therefore, to optimize and obtain a sensor with a high dynamic range, a linker library on each side of the cpGFP can be engineered and variants can be screened for their responses in mammalian HEK293 cells. In addition, modulating the residues interacting with chromophores or in the binding pockets can also have profound impact on both dynamic range and affinity. In the case of dLight1, a point mutation (F129A) was introduced into a conserved residue[25] at the interface between the GPCR and G-protein binding to increase the dynamic range. Sensor affinity can be tuned by choosing to start with a different receptor subtype (Fig. 1). In fact, many neuromodulators have multiple cognate GPCR subtypes that they can bind to and activate with different affinities.

As GPCR-based sensors become increasingly popular (more sensors built using a strategy similar to ours have recently been introduced[26–28]), it is especially important that both developers and end

users utilize a common workflow to test all new sensor variants as they become available and compare them with currently existing ones. Owing to heterogeneous patterns of neuromodulator release throughout the brain, we suggest that multiple sensors with different affinities should be developed for each ligand, similar to the dLight1 family. This will increase the flexibility in choosing which sensor to use in different brain regions and experimental conditions. To maximize the chances of success, users should choose a sensor with a dynamic range and affinity deemed most appropriate for their experimental use.

A similar approach should be followed when selecting the appropriate sensor for imaging neuromodulators other than DA. Before proceeding to testing and validation of these sensors in vivo, considerations must be taken on the expected release concentrations of the neuromodulator being analyzed. To this aim, if release concentrations of the neuromodulator of interest in a particular brain region were previously measured using voltammetry or microdialysis, this information should provide a useful guide for selecting a probe with appropriate sensitivity. Finally, for each new sensor being developed, it is very important to ensure high molecular specificity, as in the case of dLight1, by verifying that the probe shows little to no response to endogenous molecules other than the cognate ligand, including its precursors and metabolites.

### Considerations for end users

To achieve an optimal SNR during in vivo imaging experiments, sensor expression must be optimized for the brain region of choice. To determine the ideal conditions for optimal sensor expression in vivo, we recommend first determining the titer of the virus and injecting in parallel various volumes and dilutions of the viral stock. Sensor expression levels can then be checked after 2–3 weeks. At that point, one practical method of quantifying the SNR for evaluating sensor performance in vivo is to use an environmental stimulus that is known to release neuromodulator of interest in a defined region (e.g., consumption of sucrose water leads to DA release in the ventral striatum) and compare the corresponding $\Delta F/F$ values. In the case of dLight1 sensors, we find that injection of 150 nl of a viral solution at $10^{11}$ viral genomes per milliliter (VG/ml) and 2 weeks' incubation time lead to expression levels sufficient for in vivo imaging experiments with acceptable $\Delta F/F$ values (~10–20% for spontaneous peaks).

Although the turnover of these sensors has not yet been fully established, the typical lack of ligand-induced internalization will most likely keep the expression levels increasing over time. This could lead to molecular overcrowding of the cell membrane and, as a consequence, some degree of toxicity to the cells, because of alteration of membrane properties. Thus, if expression times longer than 2 months are needed for experimental purposes, a careful characterization of sensor protein levels, and of the physiological properties of the expressing cells, is recommended (e.g., electrophysiological characterization of cell health and/or immunohistochemical evaluation of any late-onset inflammatory responses).

### Advantages and limitations of different dLight1 variants

When developing and using these tools, it is important to keep in mind that often there is not a 'one-size-fits-all' sensor. Instead, sensor properties (most importantly, the ligand-binding affinity) must be appropriately chosen to match the release properties of the analyte being sensed in the brain ROI. In an ideal scenario, multiple sensor variants are available so that, as a whole, they can cover a wide range of affinities and dynamic ranges to match the demands of each individual system being studied. This is the case for the dLight1 family of DA sensors (for a direct comparison of sensor properties for all members of this family, see Table 1). Although DA is recognized by five different receptor subtypes, engineering of all DA receptors into fluorescent sensors has not yet been possible because of expression issues for the DRD3 and DRD5 subtypes. However, we have successfully engineered sensors based on DRD1 (dLight1.1, 1.2 and 1.3), DRD2 (dLight1.5) and DRD4 (dLight1.4)[16]. Among these sensors, dLight1.4 has the highest affinity (dissociation constant ($K_d$) <10 nM). This sensor variant still lacks in vivo validation; however, because of its extremely high affinity, it is presumably ideal for imaging DA dynamics in brain regions receiving little DA innervation and where DA release concentrations are expected to be low (e.g., prefrontal cortex, hippocampus[29]). Other variants, such as dLight1.1, dLight1.2 and dLight1.5, have intermediate apparent affinities (100 nM < $K_d$ < 1,000 nM) and are thus considered suitable for use in multiple brain regions. Of these variants, dLight1.5 is the only one that has yet to be validated in vivo. dLight1.1 has been validated for in vivo photometry imaging of behaviorally or optogenetically evoked DA transients in the nucleus accumbens (NAc)

**Table 1 | Comparison of all dLight1 variants available to date, including the parent dopamine receptor subtype (DRD), the maximal fluorescence response ($\Delta F/F_{max}$) and affinity for dopamine**

| dLight1 variant | GPCR subtype | $\Delta F/F_{max}$ | Affinity |
|---|---|---|---|
| dLight1.1 | DRD1 | 230% | 330 nM |
| dLight1.2 | DRD1 | 340% | 770 nM |
| dLight1.3a | DRD1 | 660% | 2,300 nM |
| dLight1.3b | DRD1 | 930% | 1,600 nM |
| dLight1.4 | DRD4 | 170% | 4 nM |
| dLight1.5 | DRD2 | 180% | 110 nM |

Both the maximal fluorescence response and the affinity values were determined in vitro on HEK293 cells, as reported in ref. [16].

and has already been successfully used by different laboratories[16,30–32]. dLight1.2 has been validated for two-photon imaging in the mouse cortex, where it revealed a map with functionally heterogeneous DA release events at high spatial resolution[16]. A key advantage of dLight1.1 and dLight1.2 is their fast kinetics. In fact, in brain slices, the dLight1.2 sensor was determined to respond with ~10 ms and ~90 ms activation and inactivation half-life constants, respectively. Furthermore, in awake animals, when DA release was triggered by optogenetically activating $TH^+$ cells of the ventral tegmental area (VTA), dLight1.1 accurately reported individual DA release events in the NAc for up to 10 Hz of light stimulation. Finally, the variants dLight1.3a and dLight1.3b have reduced affinity ($K_d$ >1,000 nM) but benefit from much-increased dynamic ranges (3–4× higher than that of dLight1.1). The relatively higher threshold of DA concentration required for activation of these sensors may make them less ideal for use in brain regions where DA release is low. However, because of their exquisitely large dynamic range, they could potentially enable the detection of DA release hotspots in vivo using one-photon or two-photon endoscopy techniques, although these applications remain to be tested.

## Comparison with other approaches

Besides the dLight1 family, another family of GPCR-based DA sensors, named GRAB-DA (based on DRD2), has also been reported[27]. Two versions of GRAB-DA were generated, one with high affinity (GRAB-DA1h; $K_d$ = 10 nM) and one with medium affinity (GRAB-DA1m; $K_d$ = 130 nM). GRAB-DA has been broadly validated for use in multiple animal organisms, including flies, fishes and mice. However, unlike dLight1, which has been shown to enable cellular-resolution imaging of DA transients in the cortex[16], GRAB-DA sensors have not been validated in vivo with two-photon microscopy.

To better guide users in sensor selection, we compared the properties of dLight1.3b and GRAB-DA1m in terms of basal brightness, surface expression, SNR and responses to drugs in rat dissociated neuronal culture under similar experimental conditions.

Under our imaging conditions, the two sensors appeared to have similar basal brightness and surface expression at basal level, but dLight1.3b displayed an approximately fivefold higher SNR in response to DA (100 μM) as compared to GRAB-DA1m (Supplementary Fig. 3). In addition, GRAB-DA1m displayed a relatively slow off-kinetics in response to the same concentration of DRD2 antagonist applied to dLight1.3b, which is consistent with the slow kinetics measured upon electrically evoked DA release in acute brain slices. Because these observations were done under specific imaging conditions, it will be important to compare the two sensors in more detail using a broader range of ligand concentrations and in different cell types. Therefore, although our results suggest that DRD1-based dLight1.3b is a more sensitive probe than DRD2-based GRAB-DA, a thorough and direct comparison between the two probes in multiple experimental settings will be necessary to select the probe with most ideal properties for a specific experiment.

## Experimental design

### Sensor characterization in mammalian cells and neuronal culture (Steps 1–34)

To determine the expression pattern, affinity, dynamic range and molecular specificity of the sensors, one can choose to perform in situ titration of ligands in two cultured cell types: HEK293 cells and

primary hippocampal neurons (for methods on how to culture primary hippocampal neurons, see ref. [33]). HEK293 cells are the cell line of choice for genetically encoded sensor development and characterization because of the availability of simple and robust culture and transfection techniques, as well as their human origin and their long-established use for the study of GPCRs[34]. Characterization in primary cultured neurons is necessary for sensors that are intended for use in the rodent nervous system because they more closely resemble the conditions under which the sensor will be finally utilized (i.e., cell type and animal origin). For example, to determine the apparent affinity of dLight1.1, a series of DA solutions ranging from 100 pM to 10 mM will be made and used to perfuse the imaging chamber during time-lapse imaging with either a wide-field or a confocal microscope. The in situ affinity and response linearity of the sensors will be determined to see whether it will fit the range expected to be physiologically relevant for measuring DA release. To determine the specificity, a series of L-amino acids, neurotransmitters and structurally similar ligands will also be used for titration. To determine the pharmacological specificity, a series of small-molecule compounds with known pharmacological properties (i.e., efficacy and potency) for the receptor involved can be tested. To assess the photostability of the sensor, time-lapse imaging can be performed using high laser intensity for a prolonged period of time (~5–10 min). The parent FP or a previously established sensor (i.e., dLight1) can be used as benchmark control. To determine the repeatability of sensor responses during prolonged periods, as well as the linearity between the levels of ligand and maximal sensor responses, the ligand can be uncaged using an orthogonal wavelength of light (e.g., 405 nm) during imaging, assuming that a caged version of a specific ligand is available. It is necessary to repeat these steps in cultured primary neurons. We noted that sometimes sensors that express and perform well in HEK293 cells behave differently in cultured neurons. If this is the case, the best way to confront this issue is by returning to the sensor engineering step and trying some of the approaches described in Fig. 1.

The final stage of in vitro characterization consists of determining whether the sensor can interfere with endogenous cellular signaling pathways. This can be done by measuring the intracellular levels of a second messenger that, depending on the type of cognate G-protein, can be either cAMP or calcium. For sensors built on Gs- or Gi-coupled receptors, a wide array of fluorescence- or bioluminescence-based assays are currently available for measuring the levels of cAMP production induced by an agonist[35,36]. The recommended detection methods are bioluminescence based, because of the orthogonality of this method to the sensor fluorescence (firefly luciferase has an emission wavelength of 560 nm)[36]. For sensors built on Gq-coupled receptors, imaging of downstream $Ca^{2+}$ levels in combination with an orthogonal sensor is recommended (i.e., red-shifted genetically encoded calcium sensors, such as JRGECO1a[37]). Finally, it is important to test whether the sensor can engage β-arrestin. This can be tested by screening for the activity of β-arrestin as an endocytic adaptor using total-internal reflection fluorescence (TIRF) microscopy and fluorescence flow cytometry[38]. Lack of sensor clustering at the plasma membrane or internalization over a period of several minutes after the addition of agonist suggests that β-arrestin is not engaged[39,40]. To obtain reproducible and high-quality data, throughout all the in vitro experiments, it is essential to maintain cell cultures in good health and to strictly adhere to the procedures for transfection/transduction outlined in the steps below. Factors such as the number of cells plated, the timing of transfection (the number of days post-culture in the case of neurons) and the length of expression are critical to guaranteeing optimal performance of the sensor.

**Adeno-associated virus preparation**

Recombinant adeno-associated viruses (rAAVs) are the viral vectors of choice for in vivo imaging experiments with genetically encoded sensors. rAAVs can be produced at high titer with relatively small cost and fewer safety concerns as compared with alternative approaches (Box 1). Production of rAAVs for driving expression of GPCR-based sensors requires packaging of DNA encoding the sensor into viral particles. An interplay between the properties of this DNA and the type of rAAV used to package it determines the strength of sensor expression and types of cells. Careful consideration of both components can ensure that the end-product virus meets experimental needs.

Selection of appropriate rAAV precursor plasmids (pAAVs) for accepting GPCR-based sensors should include consideration of gene regulatory elements. Specifically, promoter/enhancer type, recombinase dependence and polyadenylation regulatory regions are critical to targeting specific cell types and driving appropriate levels of transgene production. Promoters can help to determine cell type specificity (e.g., pan-neuronal for hSynapsin1, pan-cellular for cytomegalovirus early enhancer/chicken beta actin; CAG) as well as transgene levels (e.g., intermediate for hSynapsin1, high for

**Box 1 | AAV cloning ● Timing 16–24 h**

**Procedure**

1 Use the molecular cloning software (Snapgene, https://www.snapgene.com/) to make a map of the target construct by copying and pasting the GPCR-based sensor open reading frame (ORF) onto the target pAAV between selected restriction sites. Remember to include the Kozak sequence. Design oligos against the resultant map to PCR-amplify the sensor ORF from its source DNA. Online programs such as OligoCalc[71] can be used to check for hairpins and homo- and heterodimers, which can reduce PCR efficiency.

2 Combine oligos and template DNA containing the sensor ORF into a polymerase master mix. Run PCR for DNA amplification in the thermocycler, following standard protocols (e.g., https://www.agilent.com/cs/library/usermanuals/public/600850.pdf). Verify the PCR product via electrophoresis on an agarose gel made with SYBR Safe. Cut a size-verified band from the gel and extract it with a gel extraction kit.

**PAUSE POINT** Purified DNA is quite stable and can be stored in an aqueous solution at 4 °C (although we recommend storing for no more than 2 weeks).

3 Digest the resultant PCR product and target pAAV vector using the selected restriction enzymes per the manufacturer's recommendations. Gel-extract the digested pAAV vector. Ligate the resultant compatible-end DNA fragments with T4 DNA ligase per the manufacturer's protocols.

4 (Optional) It is possible to dephosphorylate the digested pAAV vector DNA with alkaline phosphatase before ligation. This will prevent the possibility of the vector ligating onto itself.

5 Transform the ligated DNA into RecA-deficient competent *E. coli* per the manufacturer's recommendations and plate them onto agar plates suffused with the appropriate antibiotic. Incubate overnight at 30 °C to produce isolated clonal transformant colonies. Inoculate the desired number of transformants into LB at 30 °C overnight in an orbital shaker per miniprep protocol. Make glycerol stocks by taking a small aliquot of each culture and mixing it 1:1 with 50% (vol/vol) glycerol. Flash-freeze and store at −80 °C for up to 4 years.

6 Extract the DNA from cultures using a miniprep protocol. Send the resultant DNA for sequence verification to a commercial sequencing company (e.g., Genewiz), using either a cloning oligo or standard oligos, if available. Sequencing results can be checked for correctness by aligning to a map in molecular cloning software.

7 Amplify the correct transformant by inoculating it from glycerol stock to LB per maxi prep instructions. Be sure to grow this culture at 30 °C. Extract the DNA per endotoxin-free maxi prep protocols. With sufficient yield, the resultant DNA can be used for viral production.

**Table 2 | List of all available viral vectors for the dopamine sensor dLight1**

| dLight1 variant | Flex available? | Promoter | Addgene cat. no. |
|---|---|---|---|
| dLight1.1 | Yes | CAG, hSynapsin1 | 111067 |
| dLight1.2 | No | CAG, hSynapsin1 | 111068 |
| dLight1.3a | No | CAG, hSynapsin1 | 111055 |
| dLight1.3b | Yes | CAG, hSynapsin1 | 125560 |
| dLight1.4 | No | CAG, hSynapsin1 | 111057 |
| dLight1.5 | No | CAG, hSynapsin1 | 111058 |

Viral vectors are deposited on Addgene or directly available from the Tian laboratory. Flex, Flip excision.

CAG). Enhancers (such as the woodchuck hepatitis virus posttranscriptional regulatory element (WPRE)[41] adjust transcript production or stability, resulting in enhanced transgene production. Recombinase-dependent switches, such as the Cre recombinase–dependent FLEx switch[42], require the presence of a recombinase for expression (or potentially repression) of a transgene. This approach is a common means of targeting specific cell types, for example, in driver mouse lines that have been engineered to express recombinase in genetically defined cell populations. Finally, all mammalian expression vectors include a polyadenylation tail, which is necessary for proper transcript processing and longevity. Note that promoters and polyadenylation sites are mandatory components for all but the most specialized mammalian expression cassettes.

Genetic sequences encoding GPCR-based sensors can be directly subcloned to viral precursor plasmids by standard molecular cloning techniques. pAAVs are widely available from entities, including Addgene and most nonprofit viral vector cores. These vectors include those listed in Table 2 that we produced in the course of the characterization of dLight. As a note of caution, pAAVs contain inverted terminal repeats (ITRs) necessary for packaging of the expression cassette to viral capsids. ITRs are prone to undergoing homologous recombination when maintained in *Escherichia coli*.

As such, pAAVs must be maintained in strains engineered to be deficient for recA activity, including commercially available lines such as Stable (NEB) or Stbl3 (Thermo Fisher).

Transfer plasmids can be packaged into different capsid proteins, each conferring a different pattern of transduction and expression levels. Capsids derived from naturally occurring viral serotypes have different transduction efficiencies depending on the cell types and brain regions that receive them (for an in-depth comparison, see ref. [43]). Recent years have also seen an explosion of designer, engineered capsid types. For example, the AAV-DJ capsid[44] drives rapid and higher levels of transgene expression as compared with those derived from wild-type serotypes. Retrograde transduction can be achieved using encapsidation by retroAAV[45]. Finally, AAV9 variants synthetically evolved for systemic introduction can drive near-ubiquitous transgene expression across the central or peripheral nervous system without the use of stereotaxic surgery[46,47]. This list of capsid technologies is by no means exhaustive, but it highlights important advances made in rAAV-based gene delivery systems.

One final key to successful experiments is rAAV titers—or viable packaged capsid concentrations—used for in vivo injection. In general, the titer of a viral preparation is provided by the company contracted for producing the virus. In cases in which the titer is uncertain, it can be quantitated using qPCR in which numbers of viral genomes are determined using a standard[48]. Generally, the pAAV used in the viral production process will serve as this standard. Oligos are then designed to amplify a small segment of the incorporated expression cassette. In a qPCR method using TaqMan assays (Thermo Fisher), a probe is designed to anneal to the amplified fragment, where it is degraded, releasing a dye into a fluorescent state. A standard curve is constructed by making a serial tenfold dilution of the pAAV standard and determining cycle numbers at which samples cross a defined fluorescence threshold. Cycle numbers are then plotted against a molar concentration of the pAAV standard and fit by a log-linear regression. The cycle number from an unknown viral sample can then be used to infer genome count with a high degree of accuracy (detailed procedures are available on the Thermo Fisher website).

Although rAAV is an excellent vehicle for transgene delivery, it should be noted that other viral systems are also available for in vivo expression of GPCR-based sensors. These systems come with their own strengths and weaknesses. Notably, rabies and herpes viruses are used for driving transgene expression in cells that are synaptically connected to cells that are initially infected (reviewed in ref. [49]). Both herpes and retroviruses offer larger packaging payloads (12 to >100 kb compared to 4.4 kb for rAAV). However, use of transynaptic viruses is associated with cytomorbidity, which generally occurs within 1 month of initial infection[50,51] (see ref. [52] for methods for maintaining cell viability with rabies). Most alternative viral vectors also incur increased regulatory oversight from institutional biosafety committees and typically require biosafety level 2 facilities for their use.

**Two-photon imaging of DA release in brain slices (Step 35A)**

Characterization of performance in brain slices is a necessary intermediate step between the in vitro and in vivo validation of sensors because it provides useful information on the in situ kinetics as well as the two-photon brightness of the probe. For these experiments, one approach is to transduce the sensor DNA via AAV transfection in living animals. Different promoters (CAG, hSynapsin1), as well as flexed or non-flexed viral constructs, can be chosen for ex vivo characterization, depending on the experimental needs. Promoter selection should be done on the basis of the desired expression level and density. If a combination of different-color sensors (e.g., dLight1 together with red genetically encoded calcium or voltage sensors) is needed, it is preferable, if possible, to separate the expression of the two probes into distinct cellular types or populations, to minimize cellular stress or toxicity. To obtain information about the intensity of sensor response, as well as its spatial distribution in highly scattering brain tissue, the imaging technique of choice should be two-photon microscopy[19,53]. Once sufficient time (at least 2 weeks, in our experiments) has elapsed to allow for sensor expression, it is recommended to determine whether the sensor is sufficiently bright, as well as to determine the wavelengths affording peak dynamic range in living tissue. This can be achieved by measuring fluorescence emission spectra before and after addition of the neuromodulator to the slice perfusion.

The release of the target neuromodulator from local neuronal populations in the brain slice can often be triggered using field electrophysiological stimulation[54,55]. This is preferable to optogenetic tools because of their potential spectral overlap with the sensor excitation wavelengths. A brief (0.5-ms) single pulse of field electrical stimulation is sufficient to elicit DA release from axonal varicosities in the densely innervated striatum[55,56]. When imaging neuromodulator release from a brain slice, it is important to make sure that the electrical stimulation protocol is effective, possibly by using established approaches from the literature or by using indirect methods for detecting the

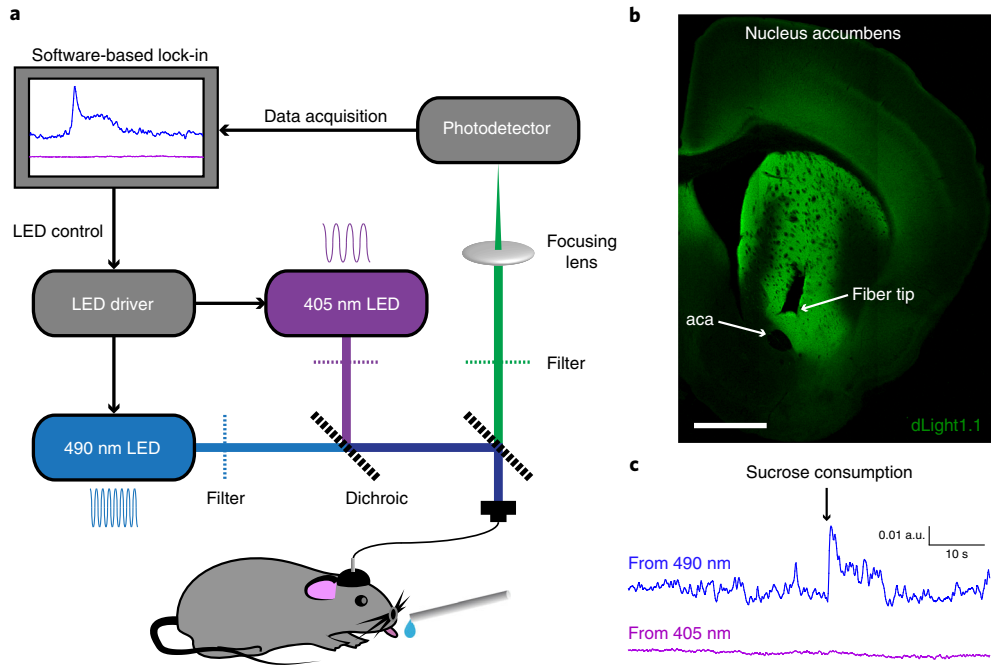


**Fig. 3 | Experimental setup for in vivo dopamine imaging with fiber photometry. a**, Schematic of fiber photometry setup described in refs. [61] and [16]. **b**, Representative histological image of dLight1.1 expressed in the nucleus accumbens core and striatum with visible fiber tip location. Scale bar, 1 mm. **c**, Spontaneous fluctuations and behavior-evoked fluorescence increase are visible from the 490-nm channel but not from the isosbestic 405-nm channel. All procedures were performed in accordance with the guidelines of the National Institutes of Health and were approved by the IACUC and the Office of Laboratory Animal Resources at the California Institute of Technology. aca, anterior commissure, anterior part; a.u., arbitrary units.

transmitter release (e.g., voltammetry[10,55], microdialysis[8] and electrophysiological recordings[57]). Application of drugs to the perfused buffer can have a profound effect on neuromodulator release. For instance, under basal conditions, the amount of DA release remains constant in response to multiple stimuli applied at different frequencies, whereas the situation dramatically changes when nicotine is applied to the slice, because this drug alters the release properties of dopaminergic axons. Because of the temperature sensitivity of the neuromodulator reuptake systems present in brain slices[58], it is important to keep the temperature as close as possible to normal physiological levels (37 °C). For a more accurate determination of the in situ kinetics of the sensor, it is necessary to use a high recording rate while imaging (preferably >100 Hz), which can be easily reached by imaging in line scan mode. This ensures that enough data points will be captured within the steep onset of fluorescence, which in the case of dLight1.1 has an on-rate of 10 ms[16]. For characterizing sensor performance during pharmacological manipulations, imaging should be performed at rates between 4 and 30 Hz, because this is a good compromise between data size and quality.

**In vivo imaging with fiber photometry or two-photon microscopy (Steps 35B–D)**

After being thoroughly characterized in vitro and/or ex vivo, genetically encoded fluorescent sensors such as dLight1 can be expressed in vivo in a brain region where DA is released (e.g., striatum or cortex) in order to monitor DA dynamics in freely moving (Fig. 3) or head-restrained animals (Fig. 6).

Fiber photometry[59] can be used to record bulk fluorescence of a sensor expressed in a single brain region without restricting the animal's movement or behavior. We have previously shown with fiber photometry that diverse environmental stimuli, such as reward-predicting cues, reward, and even liquid pump sound, can induce DA release in the NAc, as measured by dLight1 fluorescence increase (Fig. 4). In vivo imaging of sensor transients with fiber photometry can be conducted for weeks to months, therefore allowing longitudinal tracking of DA activity over various interventions (e.g., learning, disease) within a targeted neural circuit. For example, longitudinal photometry imaging across cue–reward association learning demonstrated dynamic increase of dLight1 fluorescence in response to a conditioned stimulus. Experimental procedures for long-term imaging of dLight1 start with stereotaxic injection of an AAV carrying a dLight1 variant into an ROI and surgical

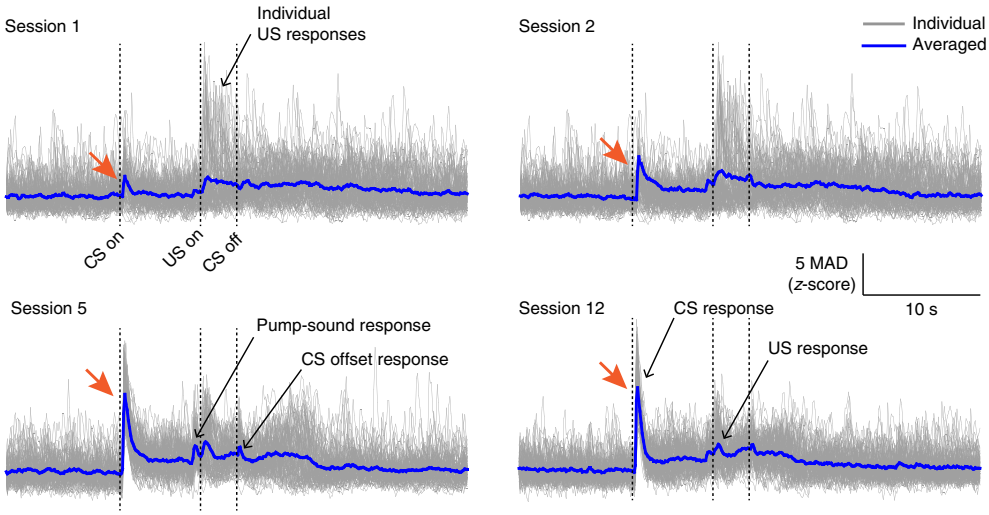


**Fig. 4 | Representative traces of dopamine dynamics during reward-based learning.** Single trial (gray) and averaged (blue) traces of dLight1.1 responses recorded from the nucleus accumbens of mice during a Pavlovian-type reward-based learning paradigm. Four representative training sessions at different time points during the learning protocol are shown. Large signal peaks are clearly visible upon conditioned stimulus (CS) onset and intensify with learning (orange arrows), as expected. Additional small peaks in the dLight1 signal are distinguishable in correspondence to pump sound for unconditioned stimuli (US, 5% sucrose) delivery and cue termination. MAD, median absolute deviation. All procedures were performed in accordance with the guidelines of the National Institutes of Health and were approved by the IACUC and the Office of Laboratory Animal Resources at the California Institute of Technology. Adapted with permission from ref. [16], American Association for the Advancement of Science.

implantation of a single optical fiber/ferrule, similar to optogenetic experiments[60]. After surgery and adequate time of waiting for viral expression (>2–3 weeks), animals expressing dLight1 can be connected to a fiber photometry setup to begin in vivo imaging while they are engaged in behavioral tasks (Supplementary Fig. 4). After imaging and behavioral experiments are finished, subjects need to be euthanized to verify dLight1 expression and exact fiber location.

To measure dLight1 transients at higher spatial resolution (e.g., to relate DA release to local cellular activity), two-photon microscopy can be used. This typically requires use of head-restrained animals, an approach that offers tight control over the animal's sensory environment, precise readout of its motor response, and the ability to perform a variety of multi-modal interrogations (e.g., combined imaging and electrophysiology or cellular-resolution optical manipulations). Use of head-restrained animals performing hundreds of stereotyped trial repetitions is particularly advantageous in the case of low-SNR sensors, because trial averaging allows even small signals to be reliably detected. In previous experiments, we have trained mice on a visuomotor association task and demonstrated functionally heterogeneous DA transients in the motor (M1) and frontal association (FrA) cortices (Fig. 6). Cellular-level ROI analysis revealed three task-relevant types of DA transients in response to locomotion, reward expectation and reward consumption, which were spatially intermingled and whose occurrence differed across cortical areas and layers.

Because current DA sensors have relatively low SNR, we recommend verifying that measured fluorescence signals result from actual changes in DA activity and not from artifactual fluctuations such as movement. This can be done by including a control group of animals expressing a sensor variant rendered incapable of binding ligand or GFP. Fluorescence transients should not be observed in these animals. To correct for movement artifacts or bleaching in dLight1 recordings, we recommend performing ratiometric measurements[61] (Fig. 3 and Supplementary Fig. 5). These can be done by including a laser/light-emitting diode (LED) and filter set for observing emissions at the sensor-independent isosbestic wavelength in fiber photometry recording. Similarly, in two-photon recordings, concomitant imaging of a co-expressed nonfunctional indicator such as tdTomato can be used to identify and at least partially correct for image artifacts caused by bleaching, tissue movement or hemodynamics. Although small image artifacts may not be apparent in single trials, averaging across trial repetitions can reveal the timing and extent of potential artifacts contributing to an ROI's response profile. Concomitant imaging of the functional and a nonfunctional indicator expressed in

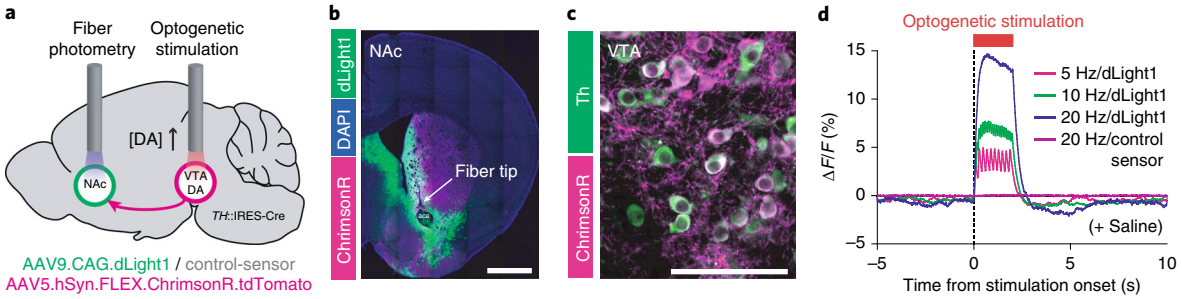


**Fig. 5 | In vivo validation of dLight1 with optogenetic control of dopamine release. a**, Schematic for fiber photometry imaging during optogenetic stimulation. In this example (related to the in vivo validation of the dopamine sensor dLight1), optogenetic excitation of dopamine release in the nucleus accumbens (NAc) is achieved by expressing the red-shifted excitatory opsin ChrimsonR[70] selectively in the dopaminergic neuronal population of the ventral tegmental area (VTA DA). Either the dopamine sensor dLight1 or a control (non-responsive) sensor was expressed in the NAc, which receives abundant projections from the VTA. Optical fibers were placed on the VTA for optogenetic excitation and on the NAc for photometry recordings. **b**, Histological verification of local expression of dLight1 (green) in NAc and ChrimsonR (magenta) in VTA projections is shown. Scale bar, 1 mm. **c**, Selective expression of ChrimsonR (magenta) in the dopaminergic population of the VTA was verified by colabeling with anti-tyrosine hydroxylase (Th) antibodies. Scale bar, 100 μm. **d**, dLight1 responses to various frequencies of optogenetic stimulation are shown. Red bar indicates duration of the optogenetic stimulation. *F*, fluorescence. All procedures were performed in accordance with the guidelines of the National Institutes of Health and were approved by the IACUC and the Office of Laboratory Animal Resources at the California Institute of Technology. Adapted with permission from ref. [16], American Association for the Advancement of Science.

the same animal, tissue region, and, ideally, the same population of cells during exactly the same behavioral trials is therefore recommended.

Depending on experimental goals, optogenetic or chemogenetic actuators can be expressed in upstream populations for manipulating DA release, or a red-shifted $Ca^{2+}$ indicator can be co-expressed with dLight1 to correlate DA dynamics with local neuronal calcium spiking[16] (Fig. 5). It is also possible to monitor sensor dynamics simultaneously from multiple regions in a single subject[62].

## Materials

### Biological materials

- HEK293 cells (ATCC, cat. no. CRL-1573) **! CAUTION** The cell lines used in your research should be regularly checked to ensure they are authentic and are not infected with mycoplasma.
- U2OS cells (ATCC, cat. no. HTB-96) **! CAUTION** The cell lines used in your research should be regularly checked to ensure they are authentic and are not infected with mycoplasma.
- Mice. For fiber photometry experiments, intracranial viral injections are performed in 8- to 24-week-old C57/Bl6 mice (The Jackson Laboratory, cat. no. 000664). For two-photon microscopy experiments in behaving mice, we recommend starting with ~6-week-old C57/Bl6 mice. By the end of head-plate implantation, virus injection, cranial window preparation, water deprivation and training, these mice will be ~11–12 weeks old, allowing imaging for several more weeks. To perform experiments involving optogenetic control of DA cells, transgenic animals expressing Cre recombinase under tyrosine hydroxylase (European Mouse Mutant Archive (EMMA), cat. no. 00254, or Jackson Laboratory, cat. no. 008601) or DA transporter (Jackson Laboratory, cat. no. 006660) can be used **! CAUTION** All experiments using animals must be approved by the institutional animal care and use committee (IACUC) or relevant regulatory body at your institution and performed in accordance with institutional and national guidelines. Permissions for the experiments shown in this protocol were obtained from the Office of Laboratory Animal Resources at the California Institute of Technology (Caltech) and from the IACUCs at Caltech and at the Salk Institute.
- Timed-pregnant 18-d gestation rat (Charles River Laboratories) **! CAUTION** All experiments using animals must be approved by the IACUC or relevant regulatory body at your institution and performed in accordance with institutional and national guidelines. Permissions for the experiments shown in this protocol were obtained from the Office of Laboratory Animal Resources at Caltech and from the IACUCs at Caltech and at the Salk Institute.
- At least 8-week-old wild-type C57BL/6J mice (The Jackson Laboratory, cat. no. 000664), for stereotaxic injection, head plate, cranial window and optical fiber/cannula implantation **! CAUTION** All experiments using animals must be approved by the IACUC or relevant regulatory body at your institution and performed in accordance with institutional and national guidelines. Permissions for the

experiments shown in this protocol were obtained from the Office of Laboratory Animal Resources at Caltech and from the IACUCs at Caltech and at the Salk Institute.

## Reagents

### Cell culture, transfection and imaging

- Hank's Balanced Salt Solution (HBSS; Life Technologies, cat. no. 14025092)
- DMEM (Thermo Fisher Scientific, cat. no. 11965-084)
- MEM; Thermo Fisher Scientific, cat. no. 11095-072)
- Opti-MEM (Life Technologies, cat. no. 31985-070)
- Lipofectamine 2000 (Life Technologies, cat. no., 11668027)
- Effectene (Qiagen, cat. no. 301425)
- DMEM (phenol red–free, serum-free, with 30 mM HEPES; Life Technologies, cat. no. 31053-028)
- Pen–strep (Thermo Fisher Scientific, cat. no. 15140122)
- FBS (Thermo Fisher Scientific, cat. no. 10082147)
- Trypsin (0.05% (wt/vol); Thermo Fisher Scientific, cat. no. 15090046)
- PBS (Thermo Fisher Scientific, cat. no. 10010023)
- PBS–EDTA (Lonza, cat. no. BE02-017F)
- Poly-D-lysine (Sigma-Aldrich, cat. no. P7280)
- Poly-L-lysine (Sigma-Aldrich, cat. no. P8920-100ML)
- Poly-L-ornithine (PLO; 0.01% (wt/vol); Sigma-Aldrich, cat. no. P0421) ▲ **CRITICAL** Prepare a 1 mg/ml PLO stock solution in ice-cold PBS, divide into aliquots and store at −20 °C (for up to 6 months) until immediately before use. Do not reuse an aliquot once it has been thawed.
- SKF 81297 (Tocris, cat. no. 1447)
- SCH 23390 (Sigma-Aldrich, cat. no. D054-5MG)
- Luciferin (GoldBio, cat. no. LUCNA-1G)
- Forskolin (Sigma-Aldrich, cat. no. F6886-25mg)
- pGloSensor-20F (Promega, cat. no. E1171)
- Alexa Fluor 647 Protein Labeling Kit (Life Technologies, cat. no. A20173)
- M1 anti-FLAG antibody (Sigma-Aldrich, cat. no. F-3040)
- Laminin (Corning, cat. no. 354232) ▲ **CRITICAL** Thaw laminin on ice, make a 500 µg/ml stock solution in ice-cold HBSS, divide into aliquots and store at −80 °C (for up to 6 months) until immediately before use. Laminin aliquots can be reused if frozen again immediately after thawing.
- UltraPure distilled $H_2O$ ($dH_2O$; Thermo Fisher Scientific, cat. no. 10977-015)
- Neurobasal medium (Thermo Fisher Scientific, cat. no. A3582901)
- B27 (50×; Thermo Fisher Scientific, cat. no. A3582801)
- GlutaMAX (100×; Thermo Fisher Scientific, cat. no. 35050061)
- Gentamicin (50 mg/ml; Thermo Fisher Scientific, cat. no. 15750060)
- 5-Fluoro-2′-deoxyuridine (FUDR; Sigma-Aldrich, cat. no. F0503) ! **CAUTION** This reagent is highly toxic and should be handled with the required personal protective equipment: type N95 dust mask (US), eye shields, face shield and gloves.
- Uridine (Sigma-Aldrich, cat. no. U3003)
- DNase (1 U/µl; Thermo Fisher Scientific, cat. no. EN0521) ▲ **CRITICAL** DNase should be stored at −80 °C (for up to 1 year).
- Dopamine HCl (Sigma-Aldrich, cat. no. H8502) ▲ **CRITICAL** Dissolve this reagent immediately before use and keep the solution on ice, because once it is dissolved, it rapidly oxidizes.
- Any plasmid encoding DRD1 under the control of a cytomegalovirus promoter (available through various vendors or labs)
- Any plasmid encoding GFP under the control of a cytomegalovirus promoter (available through various vendors or labs)

### Viral vector cloning

- pAAV vectors (see Table 2 for a list of available vectors and promoters) ▲ **CRITICAL** AAV constructs (dLight1.1, dLight1.2 and Cre-dependent, red-shifted excitatory opsin ChrimsonR are available from Addgene (cat. nos. 111067, 111068, and 62723, respectively). Viral vectors for all other dLight1 constructs can be obtained directly from the Tian laboratory. For injections in vivo, AAVs should have a titer of at least $10^{12}$ genome copies/ml.

- Oligonucleotides for sensor subcloning (Integrated DNA Technologies) Oligos for ligation subcloning are of the form 5′–[restriction site] | [start/stop codon] | [open reading frame end]-3′. As an example, dLight can be subcloned onto Addgene plasmid no. 50469 (courtesy of the lab of Bryan Roth) to put dLight1 under a CamKIIα using the forward oligonucleotide (5′-att*ggatcc*gccacc**atg**aagacgatcatcgcccctgagctac-3′ (BamHI site italicized; start codon bold)) and the reverse oligonucleotide (5′-caca*aagctt* **tca**ggttgggtgctgaccgttttgtg-3′ (HindIII site italicized; stop codon bold)) ▲**CRITICAL** For optimal translation initiation, the oligo containing the start codon must include a Kozak sequence of the form GCCRCCATGG, where ATG is the start codon itself and R indicates a degenerate purine base, A or G ▲**CRITICAL** A few base pairs should be included at the 5′ end of the oligo before the restriction site to ensure high cleavage efficiency. The number varies by restriction enzyme and can be obtained from the product information section provided by the vendor.
- Proofreading polymerase (Agilent, cat. no. 600850) ▲**CRITICAL** Polymerases, including the *Thermus aquaticus* polymerase, lack 3′–5′ exonuclease proofreading and produce ~20-fold more errors during DNA replication.
- SYBR Safe DNA Gel Stain (Thermo Fisher Scientific, cat. no. S33102)
- QIAquick Gel Extraction Kit (Qiagen, cat. no. 28704)
- Restriction enzymes (New England BioLabs, cat. no. R3104S, R3189S, R3136S) ▲**CRITICAL** Restriction enzymes are chosen based on the multiple cloning sites in the vector used.
- Quick Calf Intestinal Phosphatase kit (New England BioLabs, cat. no. M0525S)
- T4 DNA ligase (New England BioLabs, cat. no. M0202S)
- Stable competent *E. coli* line (New England BioLabs, cat. no. C3040I)
- Bacto yeast extract (Thermo Fisher Scientific, cat. no. 212750)
- Tryptone (Millipore Sigma, cat. no. T7293)
- Kanamycin sulfate (Sigma-Aldrich, cat. no. 60615)
- Ampicillin (Sigma-Aldrich, cat. no. 10835242001)
- Glycerol (Millipore Sigma, cat. no. G5516)
- QIAprep Spin Miniprep Kit (Qiagen, cat. no. 27104)
- EndoFree Plasmid Maxi Kit (Qiagen, cat. no. 12362)

**Artificial cerebrospinal fluid and brain-slicing stock solutions**

- NaCl (Thermo Fisher Scientific, cat. no. S9888)
- KCl (Sigma-Aldrich, cat. no. P9333)
- $MgCl_2$ (Sigma-Aldrich, cat. no. M8266)
- $NaH_2PO_4$ (Sigma-Aldrich, cat. no. S8282)
- $NaHCO_3$ (Sigma-Aldrich, cat. no. S5761)
- Dextrose (Sigma-Aldrich, cat. no. D9434)
- $CaCl_2$ (Sigma-Aldrich, cat. no. 449709)
- Sucrose (Sigma-Aldrich, cat. no. S0389)

**Stereotaxic injection of virus**

- Anesthesia: isoflurane (Zoetis, cat. no. 10015516) !**CAUTION** Isoflurane is an anesthetic gas with known adverse effects in humans and therefore must be handled in accordance with institutional guidelines. The use of isoflurane should be conducted in a designated area with appropriate ventilation and charcoal-based scavenging systems.
- Analgesic: buprenorphine (Sigma-Aldrich, cat. no. B9275) ▲**CRITICAL** Buprenorphine is a controlled substance, and it must be used according to institutional and governmental guidelines.
- Dexamethasone (VetOne, cat. no. NDC 13985-533-03)
- Sterile ophthalmic ointment (Dechra, cat. no. NDC 17033-211-38)
- Ethanol (Sigma-Aldrich, cat. no. 459836)
- Betadine (Thermo Fisher Scientific, cat. no. 19-027133)
- Sterile PBS (Life Technologies, cat. no. 10010023)

**Stereotaxic injection, head plate, cranial window and optical fiber/cannula implantation**

- Isoflurane (Zoetis, cat. no. 10015516)
- Analgesics: ketoprofen, 0.05 mg/kg for s.c. administration; buprenorphine SR-LAB, 0.5 mg/kg for s.c. administration) ▲**CRITICAL** Ketoprofen and buprenorphine are controlled substances and should be handled in accordance with institutional guidelines.

- Lubricant eye gel (Pharmaderm, cat. no. NDC 17033-211-38)
- Tissue adhesive (World Precision Instruments, cat. no. 503763)
- C&B Metabond (Parkell, cat. no. S380)
- Contemporary Ortho-Jet liquid, black (Lang Dental, cat. no. 1506BLK)
- Jet denture repair powder, pink (Lang Dental, cat. no. 1230PNK)
- Chlorhexidine scrub (Patterson Veterinary, cat. no. 07-888-4598)
- Chlorhexidine solution (Patterson Veterinary, cat. no. 07-839-1913)
- Ethanol (Sigma-Aldrich, cat. no. 459836)
- Ibuprofen oral suspension, USP (Akorn, cat. no. 50383-584-04)
- Hydrogen peroxide
- Super Glue
- Plates, 24-well (Falcon; Fisher Scientific, cat. no. 353047)

**In vivo fiber photometry, two-photon imaging and transcardial perfusion**

- Isopropanol (Sigma-Aldrich, cat. no. 563935)
- PBS, powder (Sigma-Aldrich, cat. no. P3813)
- Paraformaldehyde, aqueous solution (PFA; 16% (vol/vol); Electron Microscopy Sciences, cat. no. 15710)[63]

## Equipment

**Molecular cloning, cell culture, transfection and imaging**

- Tissue culture plates (10 cm and 24-well; Thermo Fisher Scientific, cat. nos. 12565020 and 12565163)
- Aluminum foil
- Glass-bottom dishes (Mattek, cat. no. P35G-1.5-14-C)
- Pipettes (Eppendorf, cat. nos. 4920000024, 4920000067, 4920000083)
- Pipette tips (Corning, cat. no. 302-04-151)
- Vortex (VWR, cat. no. 58816-121)
- Bottle-top filter (Thermo Fisher Scientific, cat. no. 158-0020)
- Automated cell counter (Thermo Fisher Scientific, cat. no. AMQAX1000)
- Mattek dishes (14 mm, glass bottom; Corning, cat. no. P35G-0.170-14-C)
- Stage adaptor (Warner Instruments, model no. SA-20KZ-AL)
- Quick Exchange Platform (for 35- 40-mm dishes; Warner Instruments, model no. QE-1)
- Eight-channel perfusion system (Automate Scientific, cat. no. 13-pp-54) For equipment setup, see Supplementary Fig. 6.
- Peristaltic pump (Cole-Palmer, cat. no. UX-77122-16)
- Confocal microscope (Zeiss, model no. 710)
- Microcentrifuge tubes (Eppendorf, cat. no. 022364111)
- Conical tubes (Greiner Bio-One, cat. nos. 227270 and 188261)
- Tabletop centrifuge (VWR, cat. no. SN08090933)
- Incubator (VWR, cat. no. 9120973)
- Petri dishes (Corning, cat. no. 351007)
- Erlenmeyer flask (Corning, cat. no. 49802L)
- Dust mask, type N95 (various vendors)
- Magnetic stirrer with magnetic stir bar (various vendors)

**TIRF microscopy**

▲ **CRITICAL** An inverted microscope with through-the-objective TIRF illumination is required. We use a customized instrument in the University of California, San Francisco, Nikon Imaging Center that is configured as follows.

- Nikon Ti microscope body fitted with PFS autofocus system, TIRF illuminator, Quad N-STORM dichroic and 100×/1.49 Apo TIRF objective
- Multi-wavelength laser launch with 488- and 640-nm sources (Keysight, model no. MLC-400B)
- Emission filter wheel with ET525/50m and ET705/72m band-pass filters (Sutter)
- EMCCD camera (Andor, model no. DU-897)
- Okolab stage-top incubator with $CO_2$ perfusion and objective heater
- NIS-Elements (https://www.microscope.healthcare.nikon.com/products/software/nis-elements) or MicroManager (https://micro-manager.org/) acquisition control software

**Flow cytometry**
- A flow cytometer capable of detecting Alexa Fluor 647 is required. We use a commercial BD FACSCalibur instrument and the Cy5 channel to detect Alexa Fluor 647 fluorescence
- Flow cytometry cluster tubes (Fisher Scientific, cat. no. 07-200-317)

**In-cell cAMP assay**
- A plate reader capable of luminescence imaging is required. We use a custom-built device to achieve truly simultaneous imaging of multiple assay wells at 37 °C, but any sensitive reader capable of acquisition speeds of >1 well/s at 37 °C should suffice. We prefer 37 °C imaging for detailed analysis, but a stronger luminescence response can be obtained at room temperature (18–22 °C) and this is adequate for basic sensor validation

**Viral vector cloning**
- Molecular cloning design software (commercial: Snapgene: https://www.snapgene.com/; freeware: Serial Cloner: http://serialbasics.free.fr/Serial_Cloner.html)
- Thermocycler (Thermo Fisher Scientific, cat. no. 4484073)
- Electrophoresis power supply (Thermo Fisher Scientific, cat. no. FBEC300XL)
- Electrophoresis chamber (Thermo Fisher Scientific, cat. no. OW-B1A-BP)
- Large blue LED transilluminator (IO Rodeo)
- NanoDrop 2000 spectrophotometer (Thermo Fisher Scientific, cat. no. ND2000)
- Orbital shaker/incubator (Thermo Fisher Scientific, cat. no. SHKE4000)

**Stereotaxic injection of virus**
- Dual small-animal stereotaxic frame (David Kopf, cat. no. 940)
- Tabletop isoflurane delivery system (VetEquip, cat. no. 901806SO)
- Surgical tools (scissors, forceps, skull scraper; Fine Science Tools)
- Cotton-tipped applicators (Thermo Fisher Scientific, cat. no. 23-400-101)
- Surgical stereoscope (Leica, cat. no. 10446294)
- Micro-drill (Foredom, cat. no. MH-170)
- Drill carbide burr (Henry Schein, cat. no. H1S-008)
- Glass pipettes and plunger (5–10 µl; Drummond, cat. no. 5-000-2010)
- Pipette puller (Sutter Instrument, cat. no. P97)
- MicroFil (World Precision Instruments, cat. no. MF28G-5)
- Syringes (1 ml; BD, cat. no. 329651)

**Brain slicing and electrophysiology**
- Large scissors (Fine Science Tools, cat. no. 14008-14)
- Fine scissors (Fine Science Tools, cat. no. 14060-10)
- Delicate bone trimmer (Fine Science Tools, cat. no. 16109-14)
- Glass Pasteur pipettes (Thermo Fisher Scientific, cat. no. 13-678-20A)
- Vibratome (Leica, cat. no. VT1200)
- Water bath incubator (Thermo Fisher Scientific, cat. no. FSGPD02)
- Stimulating electrode (Microprobes, cat. no. Pl2ST30.01A5)
- Silicon tubing (various vendors)
- Plastic valves (Nalgene, cat. no. 17223)
- Oxygen tank ($O_2/CO_2$ (95%/5%); various vendors)
- Glass Petri dishes (12 cm; Cole-Palmer, cat. no. UX-34551-02)
- Razor blades (VWR, cat. no. 55411-050)
- Cell strainers (Corning, cat. no. 352360)
- Glass bottles (150 ml and 1 liter; VWR, cat. nos. 10754-816 and 89000-240)
- Glass beakers (Corning, cat. no. 1003600)
- Ice cube mold (various vendors)

**Ex vivo two-photon imaging**
- Two-photon imaging system (Scientifica or Sutter Instrument)
- Peristaltic pump (Cole-Palmer, cat. no. UX-77122-16)
- Water bath incubator (Thermo Fisher Scientific, cat. no. FSGPD02)
- LED (488 nm; Thorlabs, cat. no. M490L4)

- Drip chamber (Harvard Apparatus, cat. no. 64-0142)
- Axon Digidata 1550B (Molecular Devices, cat. no. 1-CV-7B/EC)
- Grass stimulator (Grass TELEFA, model no. SD9)
- Stimulating electrode (AM Systems, cat. no. 564410)
- Slice holder (made in-house from cell strainers)

**In vivo two-photon imaging**

▲ **CRITICAL** We use a two-photon imaging system (Moveable Objective Microscope (MOM), Sutter Instrument) equipped with the following.

- Pulsed femtosecond Ti:sapphire laser (Coherent, model no. Chameleon Ultra II) tuned to 910 nm for dLight excitation; although this laser can also be used for concomitant excitation of other expressed proteins, such as tdTomato, a 1,040- or 1,070-nm femtosecond fiber laser (Coherent, model no. Fidelity-2) is recommended for more efficient and independently adjustable excitation of co-expressed red FPs
- Resonant scanner (~30.8 frames/s)
- Filters and dichroic beam splitters (Semrock, cat. no. FF735-DiO1 to separate near-infrared excitation from fluorescence light; Chroma Technology, cat. no. T565LPXR to separate green from red fluorescence signals; Chroma Technology, cat. nos. ET525/70M-2P and ET605/70M-2P to further filter dLight and tdTomato signals, respectively)
- GaAsP photomultiplier tubes (Hamamatsu Photonics, model no. H7422-40)
- High numerical aperture (NA) water-immersion objective lens (Nikon, model no. CFI75 LWD 16X)
- Behavior setup (custom-built; task- and brain-region dependent)
- Behavior chamber for animal training (Med-Associates, product no. ENV-016MD)
- Mini exercise ball with stand (Habitrail) and optical kit encoder (US Digital, cat. no. E7PD-720-118-D-H-G-3-E7P) attached to the exercise ball for measurement of the animal's locomotor activity
- Syringe pump for reward delivery (NE-500 programmable OEM syringe pump and OEM starter kit; New Era Pump Systems)
- LCD display for visual stimulus presentation (ICP Deutschland, cat. no. LCD-KIT121GX-R11)
- Data acquisition board (multifunction I/O device; National instruments, cat. no. PCI-6221)
- Behavior control and data acquisition system (MonkeyLogic[64]; for system requirements, see http://www.brown.edu/Research/monkeylogic/)
- Optomechanical construction parts to integrate the above components (Thorlabs)
- Data analysis and storage solutions: desktop computer with at least 128 GB RAM and an Intel i9 processor running at 3.1 GHz. Network attached storage (NAS) (Synology, cat. no. DS1817) equipped with internal hard drives of choice (e.g., Western Digital, model no. Ultrastar DC HC530)[64]

**Stereotaxic injection and optical fiber/cannula implantation**

- Dual small-animal stereotaxic frame (David Kopf, cat. no. 940)
- Tabletop isoflurane delivery system (VetEquip, cat. no. 901806SO)
- Surgical tools (e.g., scissors, forceps, spatula, and scalpel blades; Fine Science Tools)
- Cotton-tipped applicators (Thermo Fisher Scientific, cat. no. 23-400-101)
- Adjustable precision tip applicator (Parkell, cat. no. S379) or 1-ml syringes (BD, cat. no. 329651)
- Surgical stereoscope (Leica, cat. no. 10446294)
- High-speed rotary micromotor kit (Foredom, cat. no. K.1070)
- Drill bits (no. 73; Kyocera, cat. no. 105-0240.340)
- Microsyringe pump and controller (World Precision Instruments, cat. no. UMP3-3)
- NanoFil syringe (10 µl; World Precision Instruments, cat. no. NANOFIL)
- Blunt NanoFil needles (33–35 gauge; World Precision Instruments, cat. no. NF33BL-2, NF34BL-2, or NF35BL-2)
- Commercial optical fibers/ferrules for photometry purposes, fiber diameter of 400 µm and 1.25- or 2.5-mm ferrules (commercially available from Doric Lenses, Thorlabs, Prizmatix) Alternatively, customized optical fiber/ferrules using 400-µm core multimode fiber, 0.50-NA (Thorlabs, cat. no. FP400URT), multimode zirconia ferrules, 1.25 mm or 2.5 mm (Kientec Systems, cat. no. FZI-LC-L6.4-420 for 1.25 mm or FZI-SC-L6.4-420 for 2.5 mm), and low-autofluorescence epoxy (Epoxy Technology, cat. no. EPO-TEK 301). Refer to ref. [60] for details on constructing implantable optical fiber/ferrules.
- Ferrule/cannula holder (Doric Lenses, cat. no. SCH1.25 or SCH2.5)
- Plastic dust caps (Thorlabs, cat. no. CAPL or CAPF)
- Ceramic mating sleeves (Thorlabs, cat. no. ADAL1 or ADAF1)

**In vivo fiber photometry imaging in freely moving mice**

- Patch cables (commercially available from vendors above, or constructible using optical fibers and ferrules described above). Refer to ref. [60] for details on making patch cables
- Light power meter (Thorlabs, cat. nos. S130VC (sensor) and PM100D (console))
- Fiber photometry setup (commercially available from Tucker-David Technologies, Doric Lenses, Neurophotometrics; an open-source systems, developed by Owen and Kreitzer [65], is also available). For resources, please refer to http://clarityresourcecenter.com/fiberphotometry.html
- Desktop for data acquisition, with at least with an Intel core i5 processor and 4 GB of memory

**Validation of dLight1 functionality in vivo with optogenetics**

- Patch cables (commercially available from vendors above, or constructible using optical fibers and ferrules described above). Refer to ref. [60] for details on making patch cables
- Light power meter (Thorlabs, cat. nos. S130VC (sensor) and PM100D (console))
- Diode laser (635 nm; OEM Laser Systems, cat. no. RD-635-00300-CWM-SD-03-LED-0)
- TTL pulse generator (Doric Lenses, cat. no. OTPG_4)
- BNC splitter, male to double female (Allied Electronics and Automation, cat. no. BA250)

**Software**

- Snapgene (https://www.snapgene.com/)
- Zen (https://www.zeiss.com/microscopy/int/products/microscope-software/zen-lite.html)
- ImageJ (http://imagej.nih.gov/ij/download.html)
- Scanimage 5 (http://scanimage.vidriotechnologies.com/display/SIH/ScanImage+Home)
- MATLAB (https://www.mathworks.com/products/matlab.html)
- GraphPad Prism (https://www.graphpad.com/)
- MonkeyLogic (http://www.brown.edu/Research/monkeylogic/)
- Fiji (https://imagej.net/Fiji)

## Reagent setup

**HEK293 cell complete medium**

Supplement 445 ml of DMEM with FBS (50 ml) and pen–strep (5 ml). The complete medium can be stored in the refrigerator (at 4 °C) for up to 2 weeks.

**Luria Broth**

Prepare Luria broth (LB) as follows: add the following to a 2-liter Erlenmeyer flask and stir on a magnetic stirrer until mixed: 10 g of NaCl, 32 g of tryptone, 10 g of Bacto yeast extract, a large magnetic stir bar and $dH_2O$ up to 2 liters. Stir until all particulates have dissolved and the solution assumes a translucent amber tint color. Transfer the solution to four 500-ml bottles. Autoclave the filled bottles. ▲ **CRITICAL** Make sure to leave the bottle screw caps loose, so that the air pressure built up inside the bottles during the autoclaving process will not cause them to explode. Label with dates and initials. The LB can be stored under these conditions at room temperature for up to 2 months. ▲ **CRITICAL** When reusing a bottle of LB multiple times, make sure to work with it in a sterile environment, using an open flame, to avoid contamination.

**LB–agar plates**

Prepare LB–agar plates for culturing bacteria in Petri dishes as follows:

1. Add the following to a 2-liter Erlenmeyer flask and stir until mixed: 40 g of agar mix, $dH_2O$ to 1 liter and a large stir bar. Autoclave, making sure the flask is covered with aluminum foil. ▲ **CRITICAL STEP** This recipe prepares ~40 plates, using 100 × 15-mm Petri dishes. ▲ **CRITICAL STEP** Move to the next step as soon as the autoclaving is done, because leaving agar at room temperature will cause it to solidify.
2. Place the flask on a heating plate at 50 °C with stirring on for ~2 h or until hot to the touch.
3. Add 1 ml of antibiotics from a stock solution of 100 mM ampicillin or 60 mM kanamycin prepared in $dH_2O$. ▲ **CRITICAL STEP** Antibiotic stock solutions can be prepared ahead of time, divided into aliquots and stocked in a −20 °C freezer for up to 6 months.
4. Take out two fresh and sterile bags of empty plates (1 bag per liter of LB–agar) and set aside.
5. Place the plates and solution near an open flame in order to sterilize the work area.

6 Carefully pour the agar solution into plates so that the amount of liquid fills the Petri dishes half-way. Sterilize the top of the flask every two or three plates by putting it into contact with the open flame.
7 Label the plates with the specified antibiotic resistance. Leave overnight at room temperature to dry any condensation on the inside of the lid.
8 Place the plates into the original packaging, seal with labeled tape and place the bags in the refrigerator. The LB–agar plates can be stored at +4 °C for up to 1 month.

**Neuronal plating medium**
Prepare neuronal plating medium by combining the components listed in the table below. The final medium can be stored at +4 °C for up to 1 week.

| Reagent | Amount |
|---|---|
| Neurobasal medium | 92 ml |
| B27 (50×) | 2 ml |
| GlutaMAX (50×) | 1 ml |
| FBS | 5 ml |
| Gentamicin (10 mg/ml) | 10 µl |

▲ **CRITICAL** Use a bottle-top filter to filter-sterilize the final medium containing all components before use.

**Glass pipettes for viral injections**
Pull the glass pipette, using the pipette puller with the general settings listed in the table below. Glass pipettes should be pulled immediately before use.

| Parameter | Setting |
|---|---|
| HEAT | 496 |
| PULL | 60 |
| VEL | 60 |
| Delay | 120 |
| Pressure | 500 |

**Viral vectors**
Upon receipt, AAVs should be thawed on ice, divided into aliquots of the desired volume and placed at −80 °C for long-term (up to 3 years) storage.

**High-sucrose artificial cerebrospinal fluid**
Prepare 1 liter of high-sucrose artificial cerebrospinal fluid (aCSF) by combining the following components (final concentrations shown): 73 mM NaCl, 2.5 mM KCl, 2 mM $MgCl_2$, 1.25 mM $NaH_2PO_4$, 25 mM $NaHCO_3$, 24 mM dextrose, 0.5 mM $CaCl_2$, and 75 mM sucrose. The solution can be stored overnight at 4 °C but should be used the next day.

**Normal aCSF**
Prepare 1 liter of normal aCSF by combining the following components (final concentrations shown): 128 mM NaCl, 2.5 mM KCl, 1 mM $MgCl_2$, 1.25 mM $NaH_2PO_4$, 25 mM $NaHCO_3$, 10 mM dextrose, and 2 mM $CaCl_2$. The solution can be stored overnight at 4 °C but should be used the next day.

## Procedure

▲ **CRITICAL** We start by providing step-by-step guidelines for all the procedures necessary for a full characterization of newly developed genetically encoded fluorescent sensors for neuromodulators in cultured cells and brain slices (Steps 1–35A). Then we provide detailed procedures for validation of such sensors in awake, behaving animals using fiber photometry or two-photon imaging (Step 35B–D).

### Sensor transfection for in vitro sensor characterization

1 Culture and transfect HEK293 cells or cultured primary rat neurons, using option A or option B, respectively (see 'Experimental design' for details).

(A) **Culture and transfection of HEK293 cells** ● Timing **5–6 h (plus ~2-d sensor expression period)**

(i) Freshly prepare HEK293 cell complete medium as described in the 'Reagent setup' section.

(ii) Thaw a vial of HEK293 cells according to manufacturer's specifications and plate ~100,000 cells in a 10-cm dish containing 10 ml of pre-warmed medium.

(iii) Coat Mattek dishes with a solution of poly-D-lysine (0.1 mg/ml) in PBS. Incubate at 37 °C for at least 1 h. Wash three times with 1 ml of $dH_2O$.

(iv) When cells reach 60–80% confluency (typically after 2–3 d), remove the culture medium and gently lift them from the glass, using a 30-s treatment with 4 ml of 0.05% (wt/vol) trypsin. Plate them onto the coated Mattek dishes containing 2 ml of pre-warmed medium (40,000 cells/plate).

(v) The next day, prepare the Effectene transfection reagent, adhering to supplier specifications, and apply it drop-wise to the cells in a circular manner. The typical transfection mixture we use consists of the following:

| Component | Final amount per Mattek dish |
|---|---|
| Buffer (from Effectene kit) | 100 µl |
| Enhancer (from Effectene kit) | 3.2 µl |
| DNA (dLight plamid of interest) | 300 ng |
| Effectene reagent | 10 µl |

▲ CRITICAL STEP For best results and to reduce the toxicity of the transfection reagent toward the cells, it is important to replace the entire medium with pre-warmed medium 5–6 h after transfection.

(vi) Allow 2 d for optimal sensor expression and trafficking onto the cell surface.

(B) **Culture and transduction of cultured neurons** ● Timing **5–6 h (plus ~2-week sensor expression period)**

(i) Thaw an aliquot of PLO at room temperature, then at 37 °C for at least 30 min. Thaw an aliquot of laminin at 4 °C. Prepare a coating solution containing PLO (40 µg/ml) and laminin (5 µg/ml) in PBS.

(ii) Immediately coat only the glass bottom of the Mattek dishes with the coating solution and incubate at 37 °C overnight.

(iii) After the overnight incubation, rinse the coated glass bottom of the Mattek dishes with 1 ml of sterile $dH_2O$ four times.

▲ CRITICAL STEP Make sure to remove any trace of $dH_2O$ after the last wash.

(iv) Euthanize a timed-pregnant rat, extract the embryos (embryonic day (E)18 stage), dissect the hippocampi and dissociate the neurons as in refs. [33,66].

! CAUTION Rats should be housed according to institutional standards, and surgical tools should be cleaned and sterilized before use. All experiments using animals must be approved by the IACUC at your institution and performed in accordance with all relevant institutional and governmental guidelines.

(v) Plate 50,000 neurons per Mattek plate. Use a 1,000-µl pipette to gently deposit the neurons onto the Matrigel-coated glass bottom and perform a gentle swirling movement with the dish to evenly distribute the cells. This will be day in vitro (DIV) 0.

(vi) Place the plates in an incubator for 30–45 min to allow the cells to settle and adhere.

(vii) Carefully add 2 ml of acclimated neuronal plating medium (for recipe, see 'Reagent setup' section) to the dish. Use the side wall to reduce the flow of the solution. Every 3 d, feed the cells, by removing half of the spent medium (1 ml) and replacing it with 1 ml of acclimated neuronal plating medium.

(viii) At DIV4, add FUDR and uridine directly to the medium by performing a 1:1,000 (vol/vol) dilution from a 10-mM stock of each, to prevent non-neuronal cells from overgrowing.

(ix) At DIV6, thaw AAVs on ice and transduce the neurons by adding the AAVs directly to the medium. A final amount of $10^9$ viral particles should be added to the medium of each

Mattek plate. Allow at least 2 weeks for sensor expression. Neurons can be kept in culture for up to 6–8 weeks.

(x) Replace the entire spent medium with pre-warmed neuronal plating medium 12 h after transduction.

### In vitro sensor characterization using confocal imaging ● Timing 1–2 h (plus data analysis)

2 Rinse the Mattek dish containing either HEK293 cells or neurons three times with 1 ml of HBSS. Apply the perfusion insert and gently add 150 µl of HBSS to the cells. Connect the inlet of the insert to the eight-channel perfusion system and the outlet to the peristaltic pump-controlled suction line.

3 Prepare serial dilutions of the ligand. Start by dissolving DA in HBSS to generate a 100 µM stock. Perform serial dilutions in HBSS to cover the desired concentration range. We recommend using tenfold dilutions from 100 µM to 1 nM. To achieve this, add 100 µl from the stock solution to 900 µl of HBSS in a separate microcentrifuge tube (now 10 µM). Continue the procedure, using the most diluted solution as the new starting concentration until the titration is complete. Apply the solutions in order of increasing concentrations in six channels of the perfusion system (for equipment setup, see Supplementary Fig. 2). Fill the last channel with HBSS only, for the washing steps.
▲ CRITICAL STEP GPCR-based sensors can be used to detect either endogenous neuromodulators or pharmacological agents. In vitro titrations can be performed with the natural or synthetic ligand of choice.
▲ CRITICAL STEP When choosing a ligand, make sure that the compound is stable for at least 1 h once dissolved in solution and kept at room temperature. If the compound is unstable, take necessary precautions to avoid its decay (i.e., keep solutions on ice until immediately before use; degas the solutions if the compound is oxygen sensitive).

4 Optimize imaging parameters. To monitor the evolution of the sensor's fluorescence over time, it is necessary to perform time-lapse imaging using the confocal microscope. Make sure to adjust the laser intensity to a low enough level so that the fluorescence intensity on the cell membrane is between 30 and 60 pixel intensity units (for 8-bit images). This will ensure that the changes in fluorescence will fall within a linear range of detection.
! CAUTION Confocal microscopy involves a class 3B laser hazard. Make sure to adopt all safety precautions and use personal protective equipment to avoid eye damage.
? TROUBLESHOOTING

5 Perform time-lapse imaging during perfusion of increasing ligand concentrations. During perfusion, use the system display to manually control switching of the eight channels. Make sure to interleave a washing step (HBSS only) before each change of concentration.
▲ CRITICAL STEP Use real-time quantification (available through the Zen software) to assess whether the expected changes in fluorescence intensity occurred and to make sure that, after the washing step, the fluorescence returns to baseline levels.

6 *Data analysis*. Open the image data file in Fiji. Obtain an average of the stack, using the grouped *z*-project function. Adjust the threshold on the averaged image to selectively highlight cell membranes, then select individual cell membranes as ROIs and add them to the ROI manager. Measure the fluorescence across the time lapse within these ROIs. Calculate the fold-change in fluorescence ($\Delta F/F$) from the raw data in MATLAB, using the following formula: $\Delta F/F = F$ peak (averaged fluorescence intensity of 10 frames after addition of ligand) $- F$ basal (averaged fluorescence intensity of 10 frames before addition of ligand) / $F$ basal. Plot the maximum $\Delta F/F$ values achieved by each ligand concentration with a suitable graphing software (for example, we use GraphPad Prism 6) and use a single-site-specific binding equation to fit the data points and determine the affinity ($K_d$ value) of the sensor for this ligand.

### TIRF imaging of sensor surface expression and localization ● Timing 1–2 h (plus sensor expression time)

7 Coat Mattek glass bottom imaging dishes with 1 ml of poly-L-lysine diluted in sterile $dH_2O$ to 0.001% (wt/vol) for 1 h. Wash the dishes three times with 1 ml of sterile $dH_2O$ and allow to dry for 1 h in a tissue culture hood.

8 Plate HEK293 cells or cultured primary rat neurons and grow to 50% confluency.

9 Transfect the dishes with the sensor (N-terminally tagged with the signal sequence-Flag epitope recognized by M1 anti-Flag) using Effectene per the manufacturer's instructions (see Step 1A(v)). Add M1–Alexa Fluor 647 (antibody and dye conjugated per manufacturer's protocol) at 0.1 µg/ml

to the culture medium and leave for 15 min in an incubator to label the surface-exposed sensor. Remove the medium and add 1.8 ml of serum-free DMEM without phenol red and supplemented with 30 mM HEPES, pH 7.4.

10 Image the cells, using a TIRF microscope with PFS autofocus engaged, alternating image acquisition between 640-nm excitation/705-nm emission and 488-nm excitation/525-nm emission channels to monitor Flag epitope (sensor) and intrinsic GFP fluorescence (sensor response), collecting sequential image pairs at 0.3 Hz for 10 min to establish a baseline.

11 Add the D1 agonist SKF 81297, diluted in 200 µl of imaging medium to achieve a final concentration of 1 µM, and then image for another 10 min at 0.3 Hz to monitor ligand response. After 10 min, add the D1 antagonist SCH 23390, diluted in 200 µl of imaging medium to achieve a final concentration of 10 µM, and continue imaging for 5 more minutes at 0.3 Hz to monitor reversal of the response.

12 Perform data analysis as described in Step 6. Note that a desirable sensor (such as dLight1) remains diffusely distributed in the plasma membrane without clustering or internalization (detected in 640/705-nm fluorescence channel) over a full cycle of sensor activation and reversal (detected in the 488/525-nm channel).

### Flow cytometry to assess sensor surface expression and internalization ● Timing 3–4 h (plus cell passaging and sensor expression time)

13 Prepare three 6-cm dishes, each plated with $4 \times 10^5$ cells. After 1 d of maintenance in the incubator, the confluency will reach t~80%.

14 The next day (day 1), transfect the dishes with N-terminally FLAG-tagged D1 receptor[61], sensor or vehicle DNA with Effectene per the manufacturer's protocol. On day 2, remove the culture medium, lift the cells by adding 2–4 ml of PBS–EDTA and replate in a 6-well dish at $2.0–8.0 \times 10^5$ cells per well. Prepare one 6-well plate for each for transfection condition plus an additional plate for non-transfected cells.

▲ CRITICAL STEP Using Effectene for transfection will lead to broad expression, but will not saturate the endocytic machinery. Measurements of internalization by flow cytometry tend to overrepresent saturated signal when using other transfection techniques such as Lipofectamine. The cell density in the 6-well dish is not critical.

15 On day 4, leave three wells without agonist and add relevant agonist at a saturating concentration (e.g., 1 µM SKF 81297 for dLight1) to the other three wells. Incubate at 37 °C for 30 min and then chill the plates on ice, remove the medium and add 500 µl of 0.1 µg/ml M1–Alexa Fluor 647 conjugate in PBS supplemented with 5% (vol/vol) FBS. Incubate for 1 h at 4 °C.

16 Wash the cells two times with 1 ml of ice-cold PBS.

17 Remove the PBS and add 400 µl of PBS plus 5% (vol/vol) FBS to each well and gently agitate (900 r.p.m. shaker) for 45 min at 4 °C to physically remove the cells from the dish and to dissociate the clusters.

▲ CRITICAL STEP Do not lift the cells with PBS–EDTA, because the M1 antibody is calcium sensitive and will dissociate.

18 Transfer the cells to Corning cluster tubes on ice. Measure the surface level of receptors with a BD FACSCalibur flow cytometer for all conditions, including the no-transfection control. Subtract the background non-transfected conditions from the transfected conditions and then divide the measurements of agonist-treated conditions by non-agonist-treated conditions to calculate the percentage of receptor remaining on the cell surface. Note that a desirable sensor will exhibit surface expression that remains stable over time and in the presence of agonist.

### cAMP assay ● Timing 3–4 h (plus sensor expression time)

19 Plate HEK293 or U2OS cells on 10-cm dishes and grow them to 80% confluency. Use HEK293 when the objective is to compare cAMP production between a receptor and a sensor. Use U2OS cells when the objective is to monitor the effect of sensor expression on cAMP production by endogenously expressed DA D1 receptors.

▲ CRITICAL STEP HEK293 cells do not express DA receptors, which makes them useful for assessing potential signaling activity of the sensors relative to expressed D1 receptor over a null background. U2OS cells express endogenous D1 DA receptors, which makes them useful for obtaining an endogenous cAMP response to D1 agonist and assessing effects of dLight1 on an endogenous cAMP response.

20 For each dish, transfect 2 μg of pGloSensor-20F, together with 1 μg of plasmid encoding sensor, parental GPCR (DRD1 for dLight1) or GFP using 10 μl of Lipofectamine 2000. This corresponds to ~10% of the amount recommended in manufacturer's protocol. We have found that transfecting larger amounts of pGloSensor-20F produces toxicity and loss of signal. The typical transfection mixture we use consists of the following:

| Component | Final amount per 10-cm dish |
|---|---|
| Lipofectamine 2000 | 10 μl |
| Opti-MEM | 2 × 1.5 ml |
| DNA | 3 μg |

▲ **CRITICAL STEP** Using Lipofectamine for transfection will lead to a high level of expression, which is useful for obtaining a strong GloSensor response.

21 On the day of the luminescence assay, remove the culture medium and lift the cells from the 10-cm dish by adding 2–4 ml of PBS–EDTA. Spin the cells down at 1,000*g* for 5 min at room temperature and resuspend in 4 ml of medium composed of DMEM without phenol red or serum and supplemented with 30 mM HEPES. Add 1.6 mM luciferin and distribute the cells at 250 μl/well into a 24-well dish. Prepare enough wells to have two technical replicates for each condition, and preincubate at 37 °C for 45 min to 1 h to equilibrate the luciferin concentration in the cells.

22 Add ligand (1 μM SKF 81297) just before measuring the luminescence values in the plate reader. For each condition, the ligand is added at 2× the final concentration in 250 μl per well of the same phenol red–free DMEM. To each plate, 20 μM forskolin is added in the same way (10 μM final concentration), producing two reference wells per plate to use for signal normalization.

23 Measure the luminescence values for agonist-treated conditions at their peaks and normalized with reference to 10-μM forskolin at its peak. Note that the above assay is specific for characterizing sensors derived from GPCRs that natively stimulate adenylyl cyclase, such as dLight1, which is based on DRD1. A desirable sensor will not produce a cAMP response on its own, as assessed using the D1 agonist SKF 81297 in HEK293 cells that do not endogenously express DRD1. A desirable sensor will also not perturb the endogenous DRD1–cAMP response, assessed in U2OS cells (which natively express DRD1) by SKF 81297 concentration–response analysis.

### Stereotaxic injection of virus ● Timing 1–2 h (plus ≥2-week virus incubation period)

24 If AAV constructs containing the GPCR-based sensor of interest are not yet available, prepare these as described in Box 1.

▲ **CRITICAL STEP** Before injection into living animals, we recommend testing the AAVs in cultured cells. For CAG-promoted viruses, apply 1 μl of undiluted, 1:10 diluted and 1:100 diluted virus directly to the media of three separate Mattek dishes containing 40% confluent HEK cells. Check under confocal microscopy for sensor expression 48 h later. For synapsin-promoted viruses, use the transduction procedure outlined in Step 12. Check sensor expression 2 weeks after transduction.

25 Anesthetize mice with 3–5% (wt/vol) isoflurane. Maintain anesthesia with 1.5–2% (wt/vol) isoflurane.

! **CAUTION** Adhere to institutional and national guidelines for animal housing and surgery. All animal experiments must be approved by the relevant IACUC.

▲ **CRITICAL STEP** Make sure that the mouse is under deep anesthesia by testing for the absence of a toe-pinch reflex.

26 Position a heating pad on top of the surgery area and under the animal. Apply lubricant eye gel to prevent excessive drying of the eye.

▲ **CRITICAL STEP** Ensure that the animal's head is stably held in place.

27 Shave the mouse head and sterilize it with iodine solution (Betadine) followed by 70% (vol/vol) ethanol. Inject an analgesic (i.e., buprenorphine, 0.3 mg/ml) subcutaneously under the scalp to reduce post-operative discomfort.

28 Cut an incision in the scalp over the skull midline and expose the skull.

29 Use hydrogen peroxide-soaked cotton swabs to clean the area and then dry it with new cotton swabs.

30 Identify the bregma and lambda under a stereoscope and level the skull using anterior–posterior and medial–lateral tilts on the stereotaxic frame. Use the tip of the drill to place the bregma and lambda in the same dorsal–ventral axis. Move the drill 1.5 mm to the left and right from the

midline to level the medial–lateral axis. Move to the proper coordinates on the skull (coordinates can be obtained from ref. [67]).

31 Make a small craniotomy hole in the target region (~0.5-mm diameter).

32 Thaw the virus on ice and prepare the injection needles as described in the 'Reagent setup' section. ▲ **CRITICAL STEP** Viral preparations can be very sensitive to freeze–thaw cycles. Whenever a new virus is made or purchased, it needs to be immediately divided into small aliquots. The tubes should then be snap-frozen by immersion in liquid nitrogen to reduce chances of damage to the viral protein components.

33 Inject an appropriate dilution and amount of the virus into the desired region at a rate of ≤100 nl/min, using the table below. Wait for 5 min for the virus to diffuse into the target brain area.

| Experiment type | Recommended parameters | | |
|---|---|---|---|
| | Promoter | Dilution | Amount |
| In vitro imaging (cultured neurons) | Synapsin | Undiluted | 1 µl |
| Ex vivo imaging (brain slices) | CAG/synapsin | 1:2–1:5 | 150 nl |
| In vivo imaging (photometry) | CAG/synapsin | 1:2–1:5 | 150 nl |
| In vivo imaging (two-photon microscopy) | CAG/synapsin | Up to 1:10 | 200–400 nl |

▲ **CRITICAL STEP** The amounts of virus to be used are indicated based on a starting concentration of $10^{13}$ VG/ml. Different dLight1 variants (Table 1) can be selected on the basis of the experimental needs and conditions.

34 Carefully retract the injection needle from the brain and seal the animal's scalp with Super Glue. Remove the animal from the surgery area, place it on a heating pad and monitor it until normal breathing is restored. Place the animal back into the home cage. Wait for 2 weeks for sensor expression before moving on to the next steps.
▲ **CRITICAL STEP** Monitor the animal daily in the week following the surgery for any irritation or inflammation of the scalp. If necessary, administer anti-inflammatory drugs (i.e., dexamethasone 2 mg/kg, delivered intraperitoneally).

## Ex vivo and in vivo validation procedures

35 The AAV-injected mice can be used for a range of ex vivo and in vivo validation procedures. For two-photon imaging of electrically stimulated DA release from brain slices, follow option A. For in vivo fiber photometry imaging of dLight1 in freely moving mice, follow option B. For validation of dLight1 functionality in vivo with optogenetics, follow option C. For in vivo two-photon imaging in behaving mice, follow option D.

(A) **Two-photon imaging of electrically stimulated DA release from brain slices** ● **Timing 5–6 h (plus reagent preparation for brain slicing)**

(i) Prepare the setup on the day before slicing, as follows. Connect the $O_2/CO_2$ (95%/5%) tank to the various chambers where the slices will be kept by using silicon tubing, plastic valves and tape (where necessary). Make sure one loose end can easily reach the cutting chamber of the vibratome for providing oxygen to the aCSF solution during slicing. Bubble ~100 ml of high-sucrose aCSF with $O_2/CO_2$ gas mixture for at least 30 min prior to pouring into an ice cube mold, and store overnight at −20 °C.

(ii) The next day, insert a new blade into the vibratome and set the water bath temperature to 32 °C (allow at least 1 h to reach the temperature). Tape four cell strainers to the glass beaker's inner wall, below the 150-ml notch. The strainers will serve as slice holders. Remove high-sucrose aCSF from 4 °C and pour ~150 ml into the glass beaker inserted with the cell strainers. Place one gas tube into the beaker and tape it in place; move the beaker into the water bath incubator to adjust to the 32 °C temperature. Fill a bucket with ice and put it on the table near the vibratome. Place gas tubes into the two 12-cm glass Petri dishes, tape in place and place them on the ice to cool. Pour ~100 ml of high-sucrose aCSF into each dish. Put one gas tube into the glass bottle with the leftover high-sucrose and place the bottle into the ice bucket to cool. Turn on the gas and oxygenate the high-sucrose aCSF with an $O_2/CO_2$ gas mixture for at least 30 min.

(iii) Anesthetize the animal with 5% (wt/vol) isoflurane and quickly extract the brain. Place the head in ice-cold high-sucrose aCSF. Leave it submerged for 10 s to chill.

(iv) While making sure the head remains submerged at all times, use fine scissors to open the skin and cut the muscle from the brain stem. Cut open the bone around the brain stem with a delicate bone trimmer and cut open the skull from the caudal end up to the olfactory bulbs. Cutting should be done along the edge of the skull, making sure no damage is done to the brain. Remove the cerebellum and brain stem with a spatula, and—extremely gently—reach under the brain and scoop it out of the skull.

(v) Obtain coronal brain slices containing the region that received the AAV injection (i.e., for DA imaging of the striatum) as follows: spread enough Super Glue on the cutting plate in the chamber. Use a spatula to put the brain into contact with the paper towel to drain the excess of high-sucrose aCSF and then position the brain on the glue in an upright position (i.e., with forebrain on top and hindbrain on bottom in contact with the glue). Make sure the ventral side is facing away from the blade. Gently pour the ice-cold high-sucrose aCSF into the sink until all the brain is submerged. Place the gas tube and two ice cubes of high-sucrose aCSF into the chamber. Lower the blade to the surface of the brain and start the slicing to obtain 300-μm brain slices. The speed of the blade should be set to 0.14 mm/s and the amplitude to 1.5 mm. Once the striatum becomes visible, start collecting the slices. Use a glass Pasteur pipette to transfer them to the cell strainers containing aCSF at 32 °C. At this point, the slices should be left to recover for ~30 min, at which point they can be used for the experiments.

(vi) Prepare the two-photon perfusion system setup. Place a 50-ml syringe ~80 cm higher than the recording chamber and connect the syringe and chamber with silicon tubing. Pour ~40 ml of aCSF into the syringe and put one gas tube into it to oxygenate the aCSF with an $O_2/CO_2$ gas mixture for at least 30 min. Using a drip chamber connected to the tubing, adjust the perfusion speed to 5 ml/min. Connect the two-photon imaging system and the Grass SD9 stimulator to the Axon Digidata 1550B. Generate the desired stimulation protocol in Clampex to trigger imaging and stimulation by the Digidata 1550B.
▲ **CRITICAL STEP** To measure physiological responses that are as close as possible to the conditions present in an intact animal, the temperature of the perfusion system must be kept as close as possible to 37 °C. This can be achieved by submerging the reservoir of aCSF for the perfusion system in a temperature-controlled water bath, which will allow it to reach and maintain the correct temperature.

(vii) Use a glass Pasteur pipette to transfer the slices one by one to the recording chamber and gently apply the slice holder to the slice to stabilize it. Place the stimulating electrode on the micromanipulator. Using the 5× objective and LED light (488 nm), identify the slice region where the sensor expression looks optimal and move the stimulating electrode near it. Run the Clampex protocol to stimulate the slice while performing two-photon imaging.
**? TROUBLESHOOTING**

(viii) After opening the imaging data file in Fiji, run 'Image' > 'Stacks' > 'Plot *Z*-axis profile' to get the time-resolved fluorescence profile. Save the data as an Excel file. The fluorescence fold-change ($\Delta F/F$) can be calculated in MATLAB as follows. First, copy the values from the Excel file to a clear variate in MATLAB (the first column shows sampling number and the second column shows fluorescence intensity). Divide the sampling number by the sampling frequency (30 Hz), to obtain the sampling time. Calculate the mean fluorescence intensity of the first 60 recorded frames before stimulation and set it as mean baseline. Subtract the mean baseline from the fluorescence intensity at each time point and then divide by mean baseline, to get the $\Delta F/F$ value.

(B) **In vivo fiber photometry imaging of dLight1 in freely moving mice** ● **Timing 2–4 h (plus data analysis)**

(i) *Optical fiber/ferrule implantation (Steps 35B(i–xi))*. After virus injection, prepare the optical fibers/ferrules. For fiber photometry, we recommend using fibers with higher NA (>0.4) than ones for optogenetic application (usually 0.2–0.4; option C). For the size of the ferrule, either 1.25 mm or 2.5 mm in diameter is acceptable. If more than two ferrules are to be implanted, 1.25-mm ones should be used. For fiber length (excluding ferrule length), we recommend using fibers 1–2 mm longer than the targeted ventral coordinate. For example, if the region of interest is 4 mm ventral from the bregma, an optical fiber of 5–6 mm would be suitable. Transmission efficiency of a given optical fiber/cannula should be measured using a power-meter. For construction of implantable optical fibers/ferrules, refer to ref. [60].

Customizable optical fibers/ferrules for photometry are commercially available from vendors such as Doric Lenses, Prizmatix or Thorlabs; these use fibers with higher NA and a low-autofluorescence epoxy.

▲ **CRITICAL STEP** It is important to use low-autofluorescence epoxy for obtaining fluorescence signals with high SNR.

(ii) Place the ferrule in the ferrule/cannula holder and mount it on the stereotaxic frame. Make sure that the angle of the fiber is perpendicular to the skull.

(iii) Move the optical fiber tip to the bregma and zero all the coordinates. Then move to the target coordinates in the anterior–posterior and medial–lateral axes.

▲ **CRITICAL STEP** Be careful not to touch the skull with the fiber tip, as it can be damaged.

(iv) Slowly lower the optical fiber through the craniotomy hole and brain (~2 mm/min) and stop ~200 μm above the virus injection target.

(v) Use cotton swabs to dry the skull. Apply a thin layer of C&B Metabond to the skull and around the implant with tip applicators. Wait for ~10 min until the C&B Metabond hardens.

(vi) Prepare a 24-well plate. Evenly mix seven parts of Jet denture repair powder and three parts of Ortho-Jet liquid inside a well. Resulting usuable dental cement should be semi-viscous and should be applied within 2–3 minutes before it is cured. Use the tip applicator or a 1-ml syringe with a 16- or 18-gauge tip to evenly apply the dental cement around the optical fiber/ferrule and to the exposed skull. Use a spatula to smooth the surface and clean around the surrounding tissue. Make sure to expose at least half of the cannula (~3 mm) from the dental cement so that the patch cables can be connected to the cannula with a sleeve. Wait for ~15 min to dry.

(vii) Glue the skin back with surgical glue.

(viii) Place a plastic dust cap to protect the implanted optical fiber/cannula.

(ix) Inject buprenorphine (0.1 mg/kg) subcutaneously to reduce pain or discomfort.

(x) Disengage the mouse from the stereotaxic frame and move it to a clean cage placed over a heating blanket for recovery. Check the status of the animal every 15 min.

(xi) Allow a minimum of 2–3 weeks for full recovery and viral expression.

(xii) *In vivo fiber photometry imaging (Steps 35B(xii–xx)*. Prepare a patch cable to connect the optical fiber/cannula to the animal's head and the photometry setup. It is desirable that the patch cable has the same diameter and NA as those of the implanted optical fiber.

(xiii) Mice need to be habituated to tethering before any behavioral experiments or recordings begin. To do this, gently grab a mouse and remove the dust cap from the implanted cannula. Connect a patch cable to the implanted fiber/cannula with a sleeve between. It is recommended to have at least two habituation sessions, each of which should take ~30 min.

(xiv) Before photometry recordings, measure the LED or laser light power at the end of the patch cable (where it is connected to the implanted fiber) with a power meter. Try to use low light intensity to reduce photo-bleaching, especially for recordings of longer duration (>1 h). We recommend using 30–50 μW for any wavelength. Remember to account for the percentage transmission of the implanted fiber. For example, if the desired LED output for a 470-nm LED is 30 μW at the end of implanted fiber (inside brain) and the transmission rate is 75%, the light output at the end of the patch cable should be 40 μW.

(xv) Clean the implanted ferrule end with lens paper soaked with isopropanol before any recording and then connect the patch cable.

(xvi) Initiate photometry recordings. Spontaneous fluctuations should be visible in signals from blue LED or laser excitation (reflecting DA activity from dLight1) but not from isosbestic wavelength excitation (see example traces in Fig. 3 and Supplementary Fig. 4). Photo-bleaching, which usually follows an exponential decay, and occasional motion-related artifacts can be observed in both the blue and isosbestic channels. A common choice of isosbestic wavelength is within the violet range (e.g., 405 nm), but red-shifted wavelengths (e.g., 560 nm) can be also used if red FP (e.g., tdTomato) is co-expressed in the same neuronal populations[68].

**? TROUBLESHOOTING**

(xvii) Because photometry recordings are commonly performed during a specific behavioral task (e.g., operant behavior, conditioning), ensure that your photometry system interacts with behavioral variables (e.g., start of behavioral session, lever presses, auditory cue onset) or another recording system (e.g., electrophysiology) using external digital or analog inputs. These

may be useful for creating peri-stimulus histograms for analyzing DA dynamics around certain behavioral events. We have previously shown with fiber photometry that diverse environmental stimuli, such as reward-predicting cues, reward and even liquid pump sound, can induce DA release in the NAc, as measured by dLight1 fluorescence increase (Fig. 4).

(xviii) Basic pre-processing strategies for fiber photometry signals, common to GCaMP and dLight1, are described in ref. [61] or ref. [16]. Recording with an isosbestic wavelength channel can be advantageous for calculating $\Delta F/F$, because fluorescence from the blue channel can be treated as 'signal' and that from the isosbestic channel as 'noise'. First, acquired fluorescence traces from 490-nm and isosbestic wavelengths can be low-pass-filtered (corner frequency of ~15 Hz but subject to change depending on sensor properties or experimental needs) using a zero-phase distortion filter. A least-squares fit is applied to the isosbestic wavelength signal to align it to the 490-nm signal. In turn, $\Delta F/F$ can be defined as (490-nm signal – isosbestic control signal after least-squares fit) / (isosbestic control signal after least-squares fit). $\Delta F/F$ can be further processed to a $z$-score using the mean and standard deviation of the entire experimental session or of the defined 'baseline' (e.g., 10 s before presentation of time-locked stimuli). Implemented and curated MATLAB codes (these can be edited depending on the data acquisition system or for your own purposes) can be found at http://github.com/GradinaruLab/dLight1.

(xix) At the end of the experiments, perfuse the mouse with ice-cold PBS and 4% (vol/vol) PFA. Gently remove the headcap, avoiding damage to the brain. Store the excised brain in 4% (vol/vol) PFA solution overnight for further fixation, followed by slicing the brain for histological confirmation of virus expression and fiber placement[16,69].

(xx) (Optional) Once the animal has been euthanized, it is possible to recover the implanted optical fiber. Place it in acetone overnight and wipe it clean with isopropanol before reuse.

(C) **Validation of dLight1 functionality in vivo with optogenetics ● Timing 1–2 h (plus data analysis)**

▲ **CRITICAL** To confirm that cells expressing dLight1 can detect DA release in vivo at high temporal resolution, optogenetic actuators can be expressed in DA-producing cells (e.g., the VTA or the substantia nigra pars compacta (SNc)) and fiber photometry can be performed in downstream regions (e.g., striatum, cortex) where DA is released. In addition to dLight1, Cre-dependent AAVs carrying red-shifted opsin (e.g., ChrimsonR, bReaChES) can be injected into the DA-producing region in transgenic mice expressing Cre recombinase under tyrosine hydroxylase (Th) or DA transporter (DAT) promoter, as described in Steps 24–34.

(i) Work with both of the animal's arms in the stereotaxic frame. Ferrules should be secured in the ferrule/cannula holders in both arms. Make sure to zero all the coordinates on both arms at the bregma before implantation.

(ii) Implant optical fibers/ferrules one by one. We recommend implanting into anterior region first. For example, if one wants to record dLight1 in the NAc while optogenetically manipulating the VTA, start with a fiber/ferrule for photometry in the NAc. Implant the ferrule into the brain and apply C&B Metabond and dental cement around the ferrule as described in Step 35B(v–vii). Repeat the procedure for a second fiber/ferrule, in the posterior region. Stop the fiber tip insertion ~400 μm above the viral injection site.

▲ **CRITICAL STEP** If two optical fiber/ferrules are to be implanted into one mouse, use 1.25-mm-size ferrules only.

▲ **CRITICAL STEP** When applying Metabond and dental cement to the anterior side, take great care not to block the second craniotomy hole for the optogenetic ferrule.

(iii) (Optional) If your stereotaxic frame has only one arm, use the lambda as a reference point for the second ferrule. This is under the assumption that the bregma and lambda were placed in the same dorsal–ventral axis as described in Step 32.

(iv) Repeat Step 35B(vii–xi) before the start of in vivo validation experiments.

(v) Prepare an additional patch cable for optogenetic stimulation. It is desirable that the diameter and NA of the patch cord be the same as those of the implanted optical fiber (usually 200- to 300-μm diameter and 0.2- to 0.4-NA for optogenetic applications).

(vi) Repeat Step 35B(xiii) with two patch cables connected to the mouse.

(vii) Repeat Step 35B(xiv–xv) for photometry. For optogenetics, we recommend using <10 mW for most opsins and <5 mW for those that require constant light exposure for inhibition (e.g., eNpHR3.0, Arch). Remember to account for the percentage transmission of the implanted fiber as well.

(viii) Apply brief (1- to 2-s) optogenetic stimulations with intervals while recording photometry and see how the dLight1 fluorescence changes in response to such perturbation. Use an external transistor-transistor logic (TTL) pulse to trigger the laser and connect one to the analog or digital input of photometry system for accurate time stamping. Try different frequencies for stimulation. For example, we have previously demonstrated that there was a robust and stimulation-frequency-dependent fluorescence increase of dLight1 when we photo-activated VTA DA cells with red-shifted opsin ChrimsonR[16] (Fig. 5).

(ix) (Optional) To make sure that these fluorescence changes are a specific result of DA binding to the receptor, additional experiments can be performed as described above, with systemic administration of pharmacological agents. For example, because dLight1 is based on the human DRD1 receptor, systemic administration of D1 receptor antagonists such as SCH-23390 can block or reduce the dLight1 fluorescence change in response to optogenetic stimulation.

(x) For data analysis, first pre-process the photometry data as described in Step 35B(xviii). Obtain $\Delta F/F$ traces around the optogenetic stimulation onsets (e.g., 5 s before onset and 10 s after onset) that are separately available through triggered TTL pulses. Mean or peak fluorescence amplitudes from baseline and stimulation epochs can be calculated and compared to validate and characterize sensor functionality.

(D) **In vivo two-photon imaging in behaving mice ● Timing 4–5 h for surgical preparation, 3–4 weeks for behavioral training and 1–2 h per recording session (plus data analysis)**

▲ **CRITICAL** Determine whether the animals can be trained on the desired task within 3–4 weeks. If this is the case, we recommend performing head plate implantation, virus injection and cranial window preparation (Steps 35D(i–iii) below) in one surgical session before the start of animal training. If training is expected to take more time, we suggest that the animals be head-plated in a first surgical session, then trained on the task, and then—once they have reached proficiency on the task—be subjected to virus injection and craniotomy, followed by a brief retraining period.

(i) *Surgical preparation and stereotaxic virus injection (Steps 35D(i–iv))*. Anesthetize the animal with isoflurane (4% (wt/vol) for induction; 1–2% (wt/vol) for maintenance). Transfer the animal to a stereotaxic frame, protect its eyes with ophthalmic ointment, and maintain its body temperature at 36–37 °C. Remove hair over the dorsal areas of the skull, disinfect the skin, and make a midline incision. Attach a head plate to the animal's skull, following the steps described in ref. [63]. We recommend using a head plate design that allows head fixation from both sides. This will reduce vibrations during cranial window surgery and minimize motion artifacts during imaging.

▲ **CRITICAL STEP** Before affixing the head plate with Metabond, be particularly thorough in cleaning, drying and roughening the skull surface. This is critical for ensuring stability of the head plate over weeks of daily training and imaging. Use the lambda and bregma as reference points to make sure that the animal's skull is level and the virus injection site(s) are correctly marked. Center the head plate over the injection site(s) to allow lateral movement of the objective during imaging.

▲ **CRITICAL STEP** If head plate implantation, virus injection and craniotomy are performed in the same surgical session, leave the skull at the center of the head plate free of cement. If virus injection and craniotomy will be performed after animal training, the skull should be covered completely with cement to prevent infection. If head plate placement requires the bregma or lambda to be covered, mark the drilling/injection location(s) before attaching the head plate.

(ii) At this point, the cement needs to dry thoroughly. Allow ~30 min before continuing with virus injection or transferring the animal back to its home cage. If virus injection is carried out right after head plate implantation, continue anesthesia and perform Steps 35D(iv–x). If animal training precedes virus injection, make sure that the animal has 1–2 d of ad lib water/food access before surgery. Under a stereoscope, drill away the cement over the designated injection and craniotomy site. If necessary, remove the cement over the bregma and lambda to confirm the injection coordinates and continue with Steps 35D(iv–x).

▲ **CRITICAL STEP** Following virus injection, keep the exposed tissue moist with saline to prevent the dura from drying.

(iii) (Optional) If two viruses need to be delivered (e.g., to express the neuromodulator sensor in one cell type and a calcium indicator in another), we recommend performing two

separate injections at the same location and depth, rather than mixing the two virus solutions before injection. Load a micropipette with the required amount of the first virus, inject as described in Step 33, and then remove the pipette. Load a new micropipette with the second virus and inject.

(iv) Implant a chronic cranial window as described in ref. [63]. This provides some flexibility in terms of imaging, which is necessary because it is difficult to predict how many days a given animal will require for training/retraining. Before data acquisition, allow some time for surgery-induced inflammatory responses to subside (typically 2–4 weeks). Evaluate optical window clarity each week under a stereoscope and exclude mice from further training if the intended imaging location experiences tissue overgrowth. Such regrowth from the bone edges can be ameliorated by excessive water deprivation, which increases the distance between the dura, coverslip and skull.

**! CAUTION** If optical window preparation is carried out right after virus injection, make sure that the procedure is performed in accordance with your institute's biosafety regulations.

(v) *Behavioral training and habituation (Steps 35D(v and vi))*. Before any training, the animals should be handled/tamed to reduce stress and facilitate learning (1–2 d). Train the animal on the desired behavioral task in a designated behavioral chamber. For each animal, adjust the training pace and approach to maximize its performance. Keep the animals on a reversed light cycle and train them during the same time of day. The final training sessions should be performed under the two-photon microscope to accustom the animal to the recording conditions (e.g., shutter or scanner noises).

**▲ CRITICAL STEP** To maximize experimental yield, we recommend careful consideration of the following aspects of the behavioral protocol: (i) training duration, (ii) reinforcement methods, (iii) mouse strain and (iv) number of trial repetitions required for sufficient statistical power. In particular, we recommend that training goals be chosen such that the animal can comfortably learn the task within 3–4 weeks. Taking into account 5–6 d for post-surgical recovery and 2–3 d for mice to reach their working weight (i.e., the weight at which they learn most efficiently under water/food deprivation), data acquisition can commence ~5–6 weeks after virus injection. Sensor expression needs to be optimized for this time window. Too-low expression prevents optical recordings, whereas too-high expression can interfere with cell function. For the injection parameters specified in Step 34, we recommend that the expression duration not exceed 2 months. To speed up learning, task design may involve use of negative reinforcement (e.g., air puff or time-out in response to incorrect trials) in addition to positive reinforcement (e.g., water/food reward for correctly performed trials). Training success may depend on mouse strain (i.e., certain transgenic lines may take longer to train). We recommend particular consideration of animal weight. Mice of lower weight need less water/food and therefore tend to perform fewer trials per training session. In addition, the surgery on these animals can be more delicate, and their skulls may still grow over the 2-month training and imaging period. Finally, it is important for the task design to weigh trial duration against the required total number of trial repetitions the animal needs to perform during a training session.

(vi) (Optional) If your behavioral task requires more than 3–4 weeks of training, virus injection and cranial window implantation can be performed after the animal has been trained to proficiency. However, bear in mind that before surgery, water/food-deprived animals must be given 1–2 d of ad lib water/food, and they must be allowed 5–6 d of recovery after the surgery. Following this interruption, most animals will need to be retrained. Retraining starts with easier task parameters, which during retraining can usually be adjusted faster than during the initial training. However, in our experience, not all animals will reach the proficiency levels they showed immediately before surgery.

(vii) *In vivo two-photon imaging (Steps35D (vii–x))*. Starting 2–3 weeks after virus injection, sensor expression should be checked under a two-photon microscope (910-nm excitation wavelength; 40- to 130-mW average laser power at the objective output, depending on imaging depth and dLight1 expression levels/duration; see also 'Equipment' section). Evaluate sensor photostability/bleaching over imaging durations necessary to acquire a sufficient number of trials for statistical analysis.

**? TROUBLESHOOTING**

(viii) Once sensor expression and mouse performance have reached acceptable levels, test the sensor's functionality under the experimental conditions.

▲ **CRITICAL STEP** Estimate the size of the recorded data. Make sure that your data acquisition, processing and storage solutions can handle the large datasets without interruption. If acquisition of large (>4 GB) data files is necessary, determine how your analysis software/hardware can best handle it (e.g., it may be necessary to export and process the data in chunks).

**? TROUBLESHOOTING**

(ix) If sensor transients can be resolved, start the full-length recordings. Consider that amount, timing and conditions of neuromodulator release may vary across brain regions and layers. We therefore recommend systematically varying imaging location and depth. This may need to be conducted over several days because the animal's performance on the task typically declines rapidly 1–1.5 h after the start of the session. To allow trial averaging and statistical comparisons, make sure that sufficient trial repetitions are recorded at each imaging location.

(x) At the end of the experiment, collect the imaged brain tissue for histological assessment, as necessary.

## Troubleshooting

Troubleshooting advice can be found in Table 3.

**Table 3 | Troubleshooting table**

| Step | Problem | Possible reason | Solution |
|---|---|---|---|
| 4 | No sensor expression is detected | Transfection of the cells may not have worked | Check the quality of the DNA used for transfection. Repeat the transfection, using newly purified and sequence-verified plasmid DNA |
| 35A(vii) | No changes in fluorescence response are detected | The area of the slice where the stimulating electrode is placed may not release sufficient amounts of the neuromodulator being analyzed | Move the stimulating electrode to a different area of the slice or to a different slice and try again |
| 35B(xvi) | No fluorescence is detected | Sensor is not expressed in the brain | Check AAV titer by qPCR. We recommend injection concentrations of at least $10^{12}$ genome copies/ml |
| | | | Try different AAV serotypes. AAV tropism may vary across regions and cell types |
| | | | Check if needles or syringes for virus injection are clogged |
| | | | Perform histological verification. In general, immunostaining of the genetically encoded sensor is not necessary, because the endogenous fluorescence of the chromophore is sufficient to allow visualization. In specific cases in which the fluorescence would be too dim or too localized to be easily visualized, it is recommended to take advantage of a FLAG-tag positioned at the N-terminal end of the sensor, for immunolabeling |
| | | Sensor is well expressed but the fiber tip is too far away from the virus-expressed region | Try to keep the dorsal–ventral axis difference between the virus injection site and fiber tip location within 200 μm |
| | | LED or laser intensity is too weak | Gradually increase the light intensity up to 150 μW. We do not recommend increasing it beyond this point |
| | | There may be obstructions in the optical path | Thoroughly, but gently, clean the fiber tip with lens paper-soaked isopropanol before any recordings. Check the patch cables because these can easily be broken |
| | It is not clear whether the fluorescence responses are real | Possible artifacts due to animal motion may be mistaken for a fluorescence response | To correct for movement artifacts in the recordings, we recommend performing ratiometric measurements. This can be done by including a laser/LED and filter set for observing fluorescence emission at the sensor isosbestic wavelength (i.e., 405 nm) during photometry recordings |
| | | | Include a group of animals expressing a control sensor variant rendered incapable of binding its ligand (e.g., |

Table continued

**Table 3 (continued)**

| Step | Problem | Possible reason | Solution |
|---|---|---|---|
| | | | dLight1 control[16]). Fluorescence transients should not be observed in these animals |
| 35D(vii) | No fluorescence is detected | The chosen virus dilution was too high, the amount injected was too small, or the expression duration was too short | Systematically vary dilution and volume of the injected virus to optimize its expression level. The time course and pattern of expression can also be adjusted by choosing a different AAV stereotype or promoter |
| | Two viruses were injected, but expression of only one can be detected | Because two-photon imaging typically uses one Ti:sapphire laser to excite multiple fluorophores, it is possible that their expression levels are too different for sensitive imaging of both. Alternatively, there may be interference between the viruses or indicators | Try injecting the respective viruses separately into different mice. Optimize the time course and level of fluorophore expression by systematically adjusting dilution and injected volume. Once both fluorophores can be imaged under the same conditions (e.g., photomultiplier settings, laser excitation power at a given depth), try combining them again |
| 35D(viii) | Fluorescence can be detected, but no functional signals are measured | Indicator transients may be too small to resolve from a single/a few trials, indicator expression level may be too high, or sensor properties such as dynamic range may be inappropriate for recording conditions | Use trial averaging to improve SNR. Try sparser sensor expression or a different sensor variant. Perform in vivo pharmacology to test sensor responsiveness or saturation using different agonist or antagonist concentrations |

## Timing

Step 1A, HEK cell transfection: 5–6 h, plus ~2-d sensor expression period
Step 1B, culture and transduction of cultured neurons: 5–6 h, plus ~2-week sensor expression period
Steps 2–6, in vitro sensor characterization using confocal imaging: 1–2 h, plus 1–2 h for data analysis
Steps 7–12, TIRF imaging of sensor surface expression and localization: 1–2 h, plus sensor expression time
Steps 13–18, flow cytometry to assess sensor surface expression and internalization: 3–4 h, plus 24–48 h for cell passaging and sensor expression time
Steps 19–23, cAMP assay: 3–4 h, plus sensor expression time
Steps 24–34, stereotaxic viral injections: 1–2 h, plus ≥2-week virus incubation
Step 35A, two-photon imaging of electrically stimulated DA release from brain slices: 5–6 h, plus 1–2 h for reagent preparation for brain slicing
Step 35B, in vivo fiber photometry imaging of dLight1 in freely moving mice: 2–4 h, plus 2–3 h for data analysis
Step 35C, validation of dLight1 functionality in vivo with optogenetics: 1–2 h, plus 2–3 h for data analysis
Step 35D, in vivo two-photon imaging in behaving mice: 4–5 h for surgical preparation, 3–4 weeks for behavioral training and 1–2 h per recording session, plus 3–4 h for data analysis
Box 1, AAV cloning: 16–24 h

## Anticipated results

We expect this protocol to provide readily applicable information to both sensor developers and end users for implementing the existing dLight1 sensors as well as new genetically encoded neuromodulator sensors based on GPCR scaffolds. It is important to consider that there is no guarantee of success for the development of ultrasensitive sensors for neuromodulators other than DA. Our sensor engineering strategy (Fig. 1) and the procedures we laid out for sensor characterization and validation (Fig. 2) simply offer a potential approach that has proven successful in the case of dLight1 sensors, for such a high-risk, high-gain project. We believe that because of the demanding SNR requirements of all in vivo imaging approaches, thoroughly characterizing the properties of newly developed sensors is necessary to make sure they are well-adapted to their intended experimental use.

Monitoring changes in sensor fluorescence with photometry as a readout for neuromodulator dynamics can be an extremely powerful method for studying how specific neuromodulators influence behavior or disease states. As an example, in Fig. 3, we provide a schematic representation of a typical photometry setup, as well as the expression in brain tissue and raw fluorescence responses to an

individual sucrose reward stimulation. Of note, both the 490-nm- and 405-nm-excited fluorescence are shown, which demonstrate clearly that transients are due to DA release and not motion artifacts.

A particular advantage of using genetically encoded sensors to monitor neurotransmitters is the ability to track changes in dynamic responses over long periods of time, which is often the case for behavioral assays involving learning. In Fig. 4, we present a complete set of traces recorded using dLight1.1 in the mouse NAc during reward-based learning. These data clearly show the evolution of DA response to a conditional stimulus over 12 d. It is easy to imagine the usefulness of applying this type of recording in the context of specific genetic backgrounds or disease phenotypes known to be associated with DA-dependent dysfunction, because they could help pinpoint the dopaminergic signature of the disease.

For a complete optical dissection of the neural circuit function, it is important that manipulation of the neural inputs, achievable with optogenetic actuators, can be combined with a readout of the neuromodulator output using dLight1-type sensors. In Fig. 5, we show how the combination of ChrimsonR expression in dopaminergic neurons of VTA and dLight1.1 expression in the NAc can be used very robustly for simultaneous manipulations and measurements of DA release. The availability of genetic mouse strains for selective expression of the excitatory opsin in the DA-releasing neuronal population was key to these results. In fact, the VTA contains a number of different

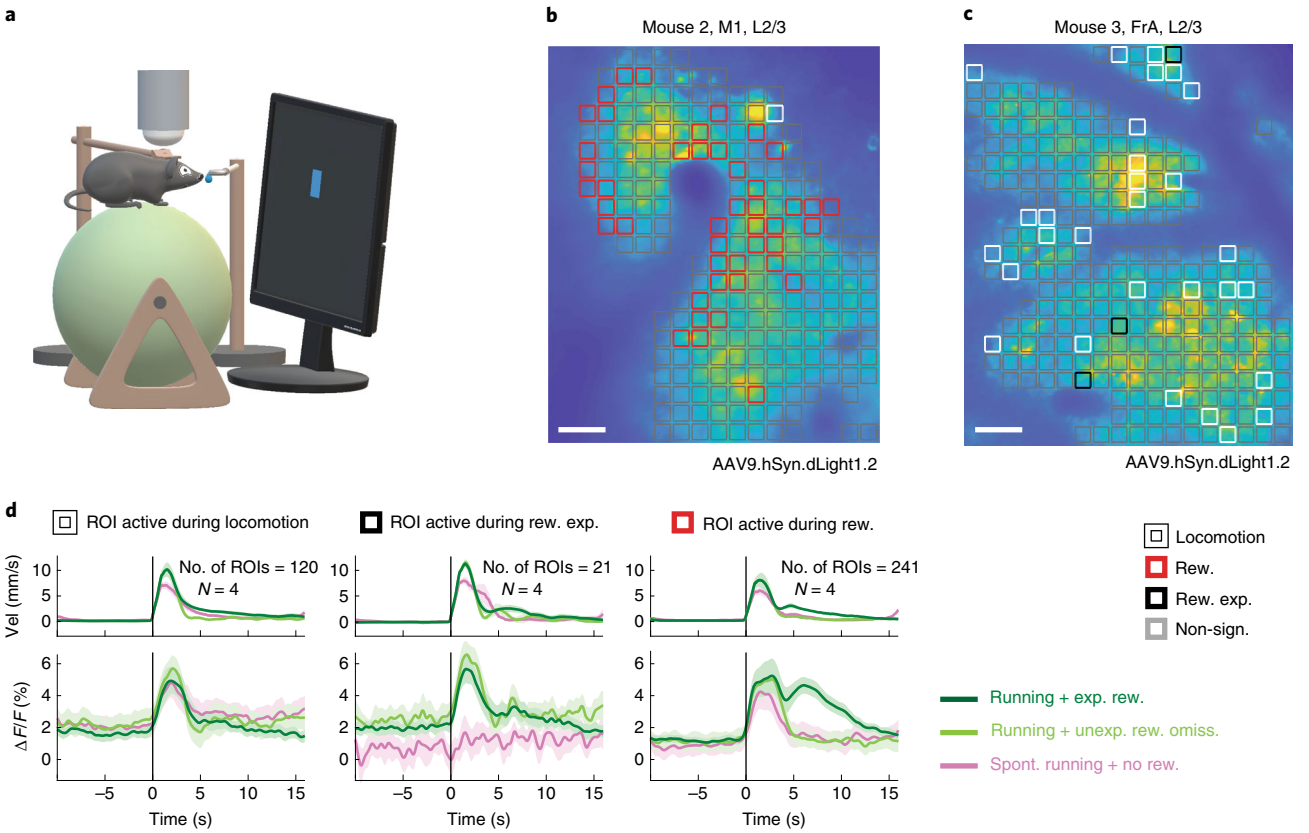


**Fig. 6 | In vivo two-photon imaging of dopamine dynamics in behaving mice. a**, Schematic of experimental setup used to record dopamine dynamics with dLight1 during a visuomotor association task. After a 10-s standstill interval, mice were visually cued to initiate a run. In 80% of correct runs, mice were rewarded with water. In 20% of randomly selected runs, the reward was withheld. Erroneous/spontaneous runs during the standstill interval led to abortion of the trial and were not rewarded. **b**,**c**, Example heatmaps from two different mice showing dLight1.2 expression level and pattern in layer (L)2/3 of M1 (**b**) and FrA cortex (**c**) 3 and 2 weeks, respectively, after stereotaxic adeno-associated viral (AAV9.hSyn.dLight1.2) vector delivery. The images are overlaid with spatially resolved ROIs (~17 µm × 17 µm) in which task-related dopamine release was investigated. Colored ROIs indicate the type of fluorescence responses observed during the task Scale bars, 50 µm. **d**, Three types of dopamine transients were identified across imaging regions. Left, ROIs responsive to locomotion independent of run context. Center, ROIs responsive to reward expectation (green traces) with no fluorescence increases during spontaneous runs (pink). Right, ROIs showing significant fluorescence increases in response to reward (dark green) but not to unexpected reward omission (light green). Population data ($N = 4$ mice; $n = 19$ recording sessions) aligned to running onset (vertical black lines). Top, mouse running velocity (Vel). Bottom, average task-related dLight1.2 transients. Shaded areas of $\Delta F/F$ traces indicate standard deviation. *F*, fluorescence; Non-sign., non-substantial; Rew., reward; Rew. exp., reward expectation. All procedures were performed in accordance with the guidelines of the National Institutes of Health and were approved by the IACUC at the Salk Institute. Adapted with permission from ref. [16], American Association for the Advancement of Science.

neurotransmitter-releasing neurons (e.g., GABA and glutamate), and thus non-selective stimulation of the VTA would have probably produced inconsistent results.

Finally, we show a specific example of how two-photon imaging of dLight1 can be used for monitoring motion or reward-relevant DA release dynamics with micron-scale spatial resolution in the cortices of head-fixed mice (Fig. 6). Obtaining spatial information on the task-dependent DA release in vivo at such high resolution is possible only with dLight1 and overcomes important limitations of analytical chemistry techniques, which provide only point-measurements. It is possible that the continued optimization of dLight1 variants in the future may lead to variants capable of producing a greater SNR for in vivo two-photon imaging.

## Reporting Summary

Further information on research design is available in the Nature Research Reporting Summary linked to this article.

## Data availability

All DNA plasmids and viruses mentioned in this protocol can be obtained from either the Tian laboratory at UC Davis or Addgene under a materials transfer agreement. All data present in this article are available from the authors upon request. Implemented and curated computer codes have been deposited in github (https://github.com/GradinaruLab/dLight1/).

## References


1. Marder, E. Neuromodulation of neuronal circuits: back to the future. *Neuron* **76**, 1–11 (2012).
2. Lee, S. H. & Dan, Y. Neuromodulation of brain states. *Neuron* **76**, 209–222 (2012).
3. Tritsch, N. X. & Sabatini, B. L. Dopaminergic modulation of synaptic transmission in cortex and striatum. *Neuron* **76**, 33–50 (2012).
4. Rusakov, D. A., Savtchenko, L. P., Zheng, K. & Henley, J. M. Shaping the synaptic signal: molecular mobility inside and outside the cleft. *Trends Neurosci.* **34**, 359–369 (2011).
5. Cachope, R. & Cheer, J. F. Local control of striatal dopamine release. *Front. Behav. Neurosci.* **8**, 188 (2014).
6. Kehr, J. & Yoshitake, T. Monitoring molecules in neuroscience: historical overview and current advancements. *Front. Biosci. (Elite Ed.)* **5**, 947–954 (2013).
7. Wightman, R. M. Detection technologies. Probing cellular chemistry in biological systems with microelectrodes. *Science* **311**, 1570–1574 (2006).
8. Darvesh, A. S. et al. In vivo brain microdialysis: advances in neuropsychopharmacology and drug discovery. *Expert Opin. Drug Discov.* **6**, 109–127 (2011).
9. Park, J., Takmakov, P. & Wightman, R. M. In vivo comparison of norepinephrine and dopamine release in rat brain by simultaneous measurements with fast-scan cyclic voltammetry. *J. Neurochem.* **119**, 932–944 (2011).
10. Bucher, E. S. & Wightman, R. M. Electrochemical analysis of neurotransmitters. *Annu. Rev. Anal. Chem. (Palo Alto Calif.)* **8**, 239–261 (2015).
11. Jaquins-Gerstl, A. & Michael, A. C. A review of the effects of FSCV and microdialysis measurements on dopamine release in the surrounding tissue. *Analyst* **140**, 3696–3708 (2015).
12. Muller, A., Joseph, V., Slesinger, P. A. & Kleinfeld, D. Cell-based reporters reveal in vivo dynamics of dopamine and norepinephrine release in murine cortex. *Nat. Methods* **11**, 1245–1252 (2014).
13. Lee, D. et al. Temporally precise labeling and control of neuromodulatory circuits in the mammalian brain. *Nat. Methods* **14**, 495–503 (2017).
14. Chen, T. W. et al. Ultrasensitive fluorescent proteins for imaging neuronal activity. *Nature* **499**, 295–300 (2013).
15. Tian, L. et al. Imaging neural activity in worms, flies and mice with improved GCaMP calcium indicators. *Nat. Methods* **6**, 875–881 (2009).
16. Patriarchi, T. et al. Ultrafast neuronal imaging of dopamine dynamics with designed genetically encoded sensors. *Science* **360**, eaat4422 (2018).
17. Venkatakrishnan, A. J. et al. Molecular signatures of G-protein-coupled receptors. *Nature* **494**, 185–194 (2013).
18. Manglik, A. & Kruse, A. C. Structural basis for G protein-coupled receptor activation. *Biochemistry* **56**, 5628–5634 (2017).
19. Svoboda, K. & Yasuda, R. Principles of two-photon excitation microscopy and its applications to neuroscience. *Neuron* **50**, 823–839 (2006).
20. Dana, H. et al. High-performance GFP-based calcium indicators for imaging activity in neuronal populations and microcompartments. *Nat. Methods* **16**, 649–657 (2019).
21. Abdelfattah, A. S. et al. Bright and photostable chemigenetic indicators for extended in vivo voltage imaging. *Science* **365**, 699–704 (2019).
22. Piatkevich, K. D. et al. Population imaging of neural activity in awake behaving mice in multiple brain regions. *Nature* **574**, 413–417 (2019).

23. Broussard, G. J. et al. In vivo measurement of afferent activity with axon-specific calcium imaging. *Nat. Neurosci.* **21**, 1272–1280 (2018).
24. Marvin, J. S. et al. An optimized fluorescent probe for visualizing glutamate neurotransmission. *Nat. Methods* **10**, 162–170 (2013).
25. Rasmussen, S. G. et al. Crystal structure of the β2 adrenergic receptor-Gs protein complex. *Nature* **477**, 549–555 (2011).
26. Jing, M. et al. A genetically encoded fluorescent acetylcholine indicator for in vitro and in vivo studies. *Nat. Biotechnol.* **36**, 726–737 (2018).
27. Sun, F. et al. A genetically encoded fluorescent sensor enables rapid and specific detection of dopamine in flies, fish, and mice. *Cell* **174**, 481–496.e19 (2018).
28. Feng, J. et al. A genetically encoded fluorescent sensor for rapid and specific in vivo detection of norepinephrine. *Neuron* **102**, 745–761.e8 (2019).
29. Mingote, S. et al. Functional connectome analysis of dopamine neuron glutamatergic connections in forebrain regions. *J. Neurosci.* **35**, 16259–16271 (2015).
30. de Jong, J. W. et al. A neural circuit mechanism for encoding aversive stimuli in the mesolimbic dopamine system. *Neuron* **101**, 133–151.e7 (2018).
31. Corre, J. et al. Dopamine neurons projecting to medial shell of the nucleus accumbens drive heroin reinforcement. *eLife* **7**, e39945 (2018).
32. Dong, H. et al. Dorsal striatum dopamine levels fluctuate across the sleep-wake cycle and respond to salient stimuli in mice. *Front. Neurosci.* **13**, 242 (2019).
33. Zhang, Y. et al. Capping of the N-terminus of PSD-95 by calmodulin triggers its postsynaptic release. *EMBO J.* **33**, 1341–1353 (2014).
34. Thomas, P. & Smart, T. G. HEK293 cell line: a vehicle for the expression of recombinant proteins. *J. Pharmacol. Toxicol. Methods* **51**, 187–200 (2005).
35. Tsvetanova, N. G. & von Zastrow, M. Spatial encoding of cyclic AMP signaling specificity by GPCR endocytosis. *Nat. Chem. Biol.* **10**, 1061–1065 (2014).
36. Thorne, N., Inglese, J. & Auld, D. S. Illuminating insights into firefly luciferase and other bioluminescent reporters used in chemical biology. *Chem. Biol.* **17**, 646–657 (2010).
37. Dana, H. et al. Sensitive red protein calcium indicators for imaging neural activity. *eLife* **5**, e12727 (2016).
38. Goodman, O. B. et al. Beta-arrestin acts as a clathrin adaptor in endocytosis of the beta2-adrenergic receptor. *Nature* **383**, 447–450 (1996).
39. Vickery, R. G. & von Zastrow, M. Distinct dynamin-dependent and -independent mechanisms target structurally homologous dopamine receptors to different endocytic membranes. *J. Cell Biol.* **144**, 31–43 (1999).
40. Irannejad, R. et al. Conformational biosensors reveal GPCR signalling from endosomes. *Nature* **495**, 534–538 (2013).
41. Lee, Y. B., Glover, C. P., Cosgrave, A. S., Bienemann, A. & Uney, J. B. Optimizing regulatable gene expression using adenoviral vectors. *Exp. Physiol.* **90**, 33–37 (2005).
42. Schnütgen, F. et al. A directional strategy for monitoring Cre-mediated recombination at the cellular level in the mouse. *Nat. Biotechnol.* **21**, 562–565 (2003).
43. Aschauer, D. F., Kreuz, S. & Rumpel, S. Analysis of transduction efficiency, tropism and axonal transport of AAV serotypes 1, 2, 5, 6, 8 and 9 in the mouse brain. *PLoS ONE* **8**, e76310 (2013).
44. Grimm, D. et al. In vitro and in vivo gene therapy vector evolution via multispecies interbreeding and retargeting of adeno-associated viruses. *J. Virol.* **82**, 5887–5911 (2008).
45. Tervo, D. G. et al. A designer AAV variant permits efficient retrograde access to projection neurons. *Neuron* **92**, 372–382 (2016).
46. Chan, K. Y. et al. Engineered AAVs for efficient noninvasive gene delivery to the central and peripheral nervous systems. *Nat. Neurosci.* **20**, 1172–1179 (2017).
47. Challis, R. C. et al. Systemic AAV vectors for widespread and targeted gene delivery in rodents. *Nat. Protoc.* **14**, 379–414 (2019).
48. Aurnhammer, C. et al. Universal real-time PCR for the detection and quantification of adeno-associated virus serotype 2-derived inverted terminal repeat sequences. *Hum. Gene Ther. Methods* **23**, 18–28 (2012).
49. Nassi, J. J., Cepko, C. L., Born, R. T. & Beier, K. T. Neuroanatomy goes viral. *Front. Neuroanat.* **9**, 80 (2015).
50. Wickersham, I. R. et al. Monosynaptic restriction of transsynaptic tracing from single, genetically targeted neurons. *Neuron* **53**, 639–647 (2007).
51. Lo, L. & Anderson, D. J. A Cre-dependent, anterograde transsynaptic viral tracer for mapping output pathways of genetically marked neurons. *Neuron* **72**, 938–950 (2011).
52. Chatterjee, S. et al. Nontoxic, double-deletion-mutant rabies viral vectors for retrograde targeting of projection neurons. *Nat. Neurosci.* **21**, 638–646 (2018).
53. Helmchen, F. & Denk, W. Deep tissue two-photon microscopy. *Nat. Methods* **2**, 932–940 (2005).
54. Palij, P. & Stamford, J. A. Real-time monitoring of endogenous noradrenaline release in rat brain slices using fast cyclic voltammetry: 3. Selective detection of noradrenaline efflux in the locus coeruleus. *Brain Res.* **634**, 275–282 (1994).
55. John, C. E. & Jones, S. R. in *Electrochemical Methods for Neuroscience* (eds Michael, A. C. & Borland, L. M.) (CRC Press/Taylor & Francis, Boca Raton, FL, 2007).
56. Bull, D. R. et al. Application of fast cyclic voltammetry to measurement of electrically evoked dopamine overflow from brain slices in vitro. *J. Neurosci. Methods* **32**, 37–44 (1990).

57. Courtney, N. A. & Ford, C. P. The timing of dopamine- and noradrenaline-mediated transmission reflects underlying differences in the extent of spillover and pooling. *J. Neurosci.* **34**, 7645–7656 (2014).
58. Xie, T., McCann, U. D., Kim, S., Yuan, J. & Ricaurte, G. A. Effect of temperature on dopamine transporter function and intracellular accumulation of methamphetamine: implications for methamphetamine-induced dopaminergic neurotoxicity. *J. Neurosci.* **20**, 7838–7845 (2000).
59. Gunaydin, L. A. et al. Natural neural projection dynamics underlying social behavior. *Cell* **157**, 1535–1551 (2014).
60. Sparta, D. R. et al. Construction of implantable optical fibers for long-term optogenetic manipulation of neural circuits. *Nat. Protoc.* **7**, 12–23 (2011).
61. Lerner, T. N. et al. Intact-brain analyses reveal distinct information carried by SNc dopamine subcircuits. *Cell* **162**, 635–647 (2015).
62. Kim, C. K. et al. Simultaneous fast measurement of circuit dynamics at multiple sites across the mammalian brain. *Nat. Methods* **13**, 325–328 (2016).
63. Goldey, G. J. et al. Removable cranial windows for long-term imaging in awake mice. *Nat. Protoc.* **9**, 2515–2538 (2014).
64. Asaad, W. F., Santhanam, N., McClellan, S. & Freedman, D. J. High-performance execution of psychophysical tasks with complex visual stimuli in MATLAB. *J. Neurophysiol.* **109**, 249–260 (2013).
65. Owen, S. F. & Kreitzer, A. C. An open-source control system for in vivo fluorescence measurements from deep-brain structures. *J. Neurosci. Methods* **311**, 170–177 (2019).
66. Chen, Y. et al. NS21: re-defined and modified supplement B27 for neuronal cultures. *J. Neurosci. Methods* **171**, 239–247 (2008).
67. Franklin, K. & Paxinos, G. *Paxinos and Franklin's the Mouse Brain in Stereotaxic Coordinates, Compact: The Coronal Plates and Diagrams* (Academic Press, 2019).
68. Menegas, W., Babayan, B. M., Uchida, N. & Watabe-Uchida, M. Opposite initialization to novel cues in dopamine signaling in ventral and posterior striatum in mice. *eLife* **6**, e21886 (2017).
69. al, J. R. C. E. Dorsal raphe dopamine neurons modulate arousal and promote wakefulness by salient stimuli. *Neuron* **94**, 1205–1219 (2017).
70. Klapoetke, N. C. et al. Independent optical excitation of distinct neural populations. *Nat. Methods* **11**, 338–346 (2014).
71. Kibbe, W. A. OligoCalc: an online oligonucleotide properties calculator. *Nucleic Acids Res.* **35**, W43–W46 (2007).


## Acknowledgements

This work was supported by NIH BRAIN Initiative grants U01NS090604, U01NS013522, DP2MH107056 and U01NS103571 (L.T.); grants DP2NS083038, R01NS085938 and P30CA014195 (A.N.); BRAIN Initiative grants U01NS013522 (J.T.W. and M.v.Z.), and NIH grant DP2NS087949 and NIH/NIA grant R01AG047664 (V.G.). K.M. is a DFG research fellow and recipient of a Catharina Foundation postdoctoral scholar award. V.G. is a Heritage Principal Investigator supported by the Heritage Medical Research Institute.

## Author contributions

T.P. and L.T. wrote the manuscript with contributions from J.R.C. and V.G. (fiber photometry and optogenetics), G.J.B. (rAAV preparation and cloning), R.L. (structural modeling), A.M. and M.v.Z. (TIRF microscopy, FACS and cAMP measurements), K.M. and A. N. (in vivo two-photon imaging in behaving mice), and J.W. (ex vivo two-photon imaging).

## Competing interests

T.P. and L.T. are co-inventors on a patent application (WO/2018/098262A1) for the technology described in this paper. L.T. is the co-founder of Seven Biosciences.

## Additional information

**Supplementary information** is available for this paper at https://doi.org/10.1038/s41596-019-0239-2.

**Correspondence and requests for materials** should be addressed to J.W. or A.N. or M.Z. or V.G. or L.T.

**Peer review information** *Nature Protocols* thanks Thomas Knopfel and other, anonymous, reviewer(s) for their contribution to the peer review of this work.

**Reprints and permissions information** is available at www.nature.com/reprints.

**Publisher's note** Springer Nature remains neutral with regard to jurisdictional claims in published maps and institutional affiliations.

Received: 11 March 2019; Accepted: 20 August 2019;
Published online: 15 November 2019

**Related link**
**Key references using this protocol**
Patriarchi, T. et al. *Science* **360**, eaat4422 (2018) https://science.sciencemag.org/content/360/6396/eaat4422/

nature research

Corresponding author(s): Mark von Zastrow, Viviana Gradinaru, Lin Tian

Last updated by author(s): 03/10/2019

# Reporting Summary

Nature Research wishes to improve the reproducibility of the work that we publish. This form provides structure for consistency and transparency in reporting. For further information on Nature Research policies, see Authors & Referees and the Editorial Policy Checklist.

## Statistics

For all statistical analyses, confirm that the following items are present in the figure legend, table legend, main text, or Methods section.

| n/a | Confirmed |
|---|---|
| ☒ | ☐ The exact sample size (*n*) for each experimental group/condition, given as a discrete number and unit of measurement |
| ☒ | ☐ A statement on whether measurements were taken from distinct samples or whether the same sample was measured repeatedly |
| ☒ | ☐ The statistical test(s) used AND whether they are one- or two-sided<br>*Only common tests should be described solely by name; describe more complex techniques in the Methods section.* |
| ☒ | ☐ A description of all covariates tested |
| ☒ | ☐ A description of any assumptions or corrections, such as tests of normality and adjustment for multiple comparisons |
| ☒ | ☐ A full description of the statistical parameters including central tendency (e.g. means) or other basic estimates (e.g. regression coefficient) AND variation (e.g. standard deviation) or associated estimates of uncertainty (e.g. confidence intervals) |
| ☒ | ☐ For null hypothesis testing, the test statistic (e.g. *F*, *t*, *r*) with confidence intervals, effect sizes, degrees of freedom and *P* value noted<br>*Give P values as exact values whenever suitable.* |
| ☒ | ☐ For Bayesian analysis, information on the choice of priors and Markov chain Monte Carlo settings |
| ☒ | ☐ For hierarchical and complex designs, identification of the appropriate level for tests and full reporting of outcomes |
| ☒ | ☐ Estimates of effect sizes (e.g. Cohen's *d*, Pearson's *r*), indicating how they were calculated |

*Our web collection on statistics for biologists contains articles on many of the points above.*

## Software and code

Policy information about availability of computer code

| | |
|---|---|
| Data collection | *Provide a description of all commercial, open source and custom code used to collect the data in this study, specifying the version used OR state that no software was used.* |
| Data analysis | MatLab computer codes are deposited in github (https://github.com/GradinaruLab/dLight1/). |

For manuscripts utilizing custom algorithms or software that are central to the research but not yet described in published literature, software must be made available to editors/reviewers. We strongly encourage code deposition in a community repository (e.g. GitHub). See the Nature Research guidelines for submitting code & software for further information.

## Data

Policy information about availability of data

All manuscripts must include a data availability statement. This statement should provide the following information, where applicable:

- Accession codes, unique identifiers, or web links for publicly available datasets
- A list of figures that have associated raw data
- A description of any restrictions on data availability

All DNA and viruses have been deposited in NCBI (accession number MH244549-MH244561), ADDGENE, and the University of Pennsylvania Vector Core. All DNA plasmids and viruses are available from UC Davis or designated repository under a material transfer agreement. Computer codes are deposited in github (https://github.com/GradinaruLab/dLight1/). All other data needed to evaluate the conclusion in the paper can be accessed using the following link: http://science.sciencemag.org/content/360/6396/eaat4422

# Field-specific reporting

Please select the one below that is the best fit for your research. If you are not sure, read the appropriate sections before making your selection.

☒ Life sciences ☐ Behavioural & social sciences ☐ Ecological, evolutionary & environmental sciences

For a reference copy of the document with all sections, see nature.com/documents/nr-reporting-summary-flat.pdf

# Life sciences study design

All studies must disclose on these points even when the disclosure is negative.

| | |
|---|---|
| Sample size | No statistical methods were used to predetermine sample size. |
| Data exclusions | No data were excluded from this study |
| Replication | Each experiment was performed on multiple cultures or animal subjects. All attempts were successful. |
| Randomization | Animals and cultures were randomly assigned for transduction with the different constructs described in the manuscript. |
| Blinding | Blinding was not used in this study. |

# Reporting for specific materials, systems and methods

We require information from authors about some types of materials, experimental systems and methods used in many studies. Here, indicate whether each material, system or method listed is relevant to your study. If you are not sure if a list item applies to your research, read the appropriate section before selecting a response.

## Materials & experimental systems

| n/a | Involved in the study |
|---|---|
| ☒ | ☐ Antibodies |
| ☒ | ☐ Eukaryotic cell lines |
| ☒ | ☐ Palaeontology |
| ☐ | ☒ Animals and other organisms |
| ☒ | ☐ Human research participants |
| ☒ | ☐ Clinical data |

## Methods

| n/a | Involved in the study |
|---|---|
| ☒ | ☐ ChIP-seq |
| ☒ | ☐ Flow cytometry |
| ☒ | ☐ MRI-based neuroimaging |

## Animals and other organisms

Policy information about studies involving animals; ARRIVE guidelines recommended for reporting animal research

| | |
|---|---|
| Laboratory animals | stated in the manuscript |
| Wild animals | *Provide details on animals observed in or captured in the field; report species, sex and age where possible. Describe how animals were caught and transported and what happened to captive animals after the study (if killed, explain why and describe method; if released, say where and when) OR state that the study did not involve wild animals.* |
| Field-collected samples | *For laboratory work with field-collected samples, describe all relevant parameters such as housing, maintenance, temperature, photoperiod and end-of-experiment protocol OR state that the study did not involve samples collected from the field.* |
| Ethics oversight | *Identify the organization(s) that approved or provided guidance on the study protocol, OR state that no ethical approval or guidance was required and explain why not.* |

Note that full information on the approval of the study protocol must also be provided in the manuscript.